Eur. Phys. J. A **1**, 317–336 (1998)

THE EUROPEAN PHYSICAL JOURNAL A

Phenomenological $\pi N \to \pi\pi N$ amplitude and analysis of low energy data on total cross sections and 1–D distributions

A.A. Bolokhov[1], M.V. Polyakov[2], S.G. Sherman[2]

[1] Sankt-Petersburg State University, Sankt-Petersburg, 198904, Russia
[2] St. Petersburg Institute for Nuclear Physics, Sankt–Petersburg, 188350, Russia

Received: 11 November 1997
Communicated by V.V. Annisovich

Abstract. We develop the phenomenological amplitude of the $\pi N \to \pi\pi N$ reaction taking into account the exchanges of Δ and $N^{(*)}$ along with the OPE mechanism and the polynomial background derived with the account of isotopic, crossing, C, P and T symmetries of strong interactions.
The data base consisting of total cross sections in the energy region $0.300 \leq P_{\rm Lab} \leq 500$ MeV/c and 1D distributions from the bubble–chamber experiments was used to determine free parameters of the amplitude. For the first time there was found an amplitude equally well describing the broad variety of different data in all reaction channels. The best solutions are characterized by $\chi^2_{\rm DF} = 1.16$, $N = 411$. The isobar exchanges are found to be more important than OPE at the considered energies. Despite this the parameters of OPE are statistically significant; however, the $\pi\pi$–scattering lengths appear different in different solutions.

PACS. 13.75.-n Hadron-induced low- and intermediate-energy reactions and scattering (energy $\leq$10 GeV) – 13.75.Gx Pion-baryon interaction – 13.75.Lb Meson-meson interaction

1 Introduction

The pion–production reactions play the important role in the low energy physics of elementary particles and nuclei. The recent results [1] of the so called Generalized ChPT approach [2] and the progress in the two–loop ChPT calculations [3,1] are claiming for more precise experimental information on the $\pi\pi$ interaction in $O(k^6)$ order. Since it is not possible to create the pionic target or the colliding pion beams there are only indirect ways for obtaining experimental data on the $\pi\pi$ scattering. The reactions $\pi N \to \pi\pi N$ and $K \to \pi\pi e\nu$ are considered as the most important sources of the indirect information on low energy characteristics of the $\pi\pi$ interaction.

Some of the planned experimental measurements of the $\pi N \to \pi\pi N$ reactions at low energies listed in [4] have already been finished: BNL and LAMPF results on total cross sections have been published [5], [6], 1D-distributions have appeared recently in WWW (home pages [7], [8]), higher distributions are in progress, the off–line treatment of experimental tapes of the TRIUMF experiment [9] will be completed soon.

The main goal of the present work is to develop the most extensive phenomenological $\pi N \to \pi\pi N$ amplitude suitable for the model–independent determination of parameters of $\pi\pi$ interaction and to use this amplutude for the analysis of the available now data in the near–threshold and the intermediate energy regions.

We are basing upon the approach [10] by Oset and Vicente–Vacas; however, the amplitude is assumed to be relativistic. We try to fix the phenomenological amplitude by fitting the data on total cross sections and distributions of the reaction in question in the energy region from threshold up to $P_{\rm Lab} \leq 500$ MeV/c.

To avoid any doubt in the results in respect to correctness of acceptances, systematic errors, etc. the distribution data are chosen to be the bubble–chamber ones. This leaves us with rather old experiments which are discussed in Sect. 3. However, the significant part of the data has never been published and its most part eluded strong theoretical analyses apart authors' checks of some isobar–like models. Therefore, it seems important to develop tools of theoretical treatment of such data for the purpose of determination of characteristics of pion–pion and pion–nucleon interactions.

It is worth noting that the considered reaction via unitarity relations is directly related to the fundamental process of elastic pion–nucleon scattering at intermediate energies and other processes like $\gamma N \to \pi\pi N$ which gain the raising interest in the ChPT approach. The reaction also enters the pion–nuclei scattering as an elementary process. Therefore, the structure of $\pi N \to \pi\pi N$ amplitude is of great importance for nuclear and particle physics.

When possible the reaction $\pi N \to \pi\pi N$ will be simply referred as $\pi 2\pi$ below.

The paper is organized as follows. The content of Sect. 2 reminds the basics of the low energy phenomenology of the $\pi 2\pi$ reaction and describes the structure of our amplitude. Section 3 provides the summary of experimental data on distributions and total cross sections which we are analyzing. Section 4 is devoted to specifics of the fitting procedure and main results of analysis. The summary, the concluding remarks and the discussion of the perspectives of the further development are given in Conclusions.

2 Model of $\pi N \to \pi\pi N$ amplitude

The principal features of the near–threshold phenomenology of the $\pi 2\pi$ reaction had been already discussed in the paper [11]. There, the smooth background amplitude and the OPE one had been derived for the energy domain bounded by the reaction threshold and the threshold $P_{\rm Lab} \approx 500$ MeV/c of the Δ–isobar creation in the final state. However, the statistically significant data on $\pi 2\pi$ distributions described in the next section, exist just for the boundary and slightly above of the pointed energy region. This makes necessary to modify the amplitude elaborated in [11] since the smoothness assumption is hardly to be valid there.

In the current section we recall the phenomenology of $\pi 2\pi$ processes to be taken into account (Subsect. 2.2) and principal parts of the modified amplitude (Subsect. 2.3) the parameters of which must be determined from the data fittings. We start with the brief description of the spin–isospin structure of the discussed amplitude.

2.1 $\pi N \to \pi\pi N$ amplitude

2.1.1 General structure

The amplitude $M^{abc}_{\beta\alpha}(\lambda_f;\lambda_i)$ of the reaction

$$\pi^a(k_1) + N_\alpha(p;\lambda_i) \;\to\; \pi^b(k_2) + \pi^c(k_3) + N_\beta(q;\lambda_f) \quad (1)$$

has 4 degrees of freedom in the isotopic space; it might be expressed either in terms of the definite isospin amplitudes or in terms of the isoscalar ones. Separating the nucleon spinor wave functions

$$M^{abc}_{\beta\alpha}(\lambda_f;\lambda_i) = \bar u(q;\lambda_f)\hat M^{abc}_{\beta\alpha}(i\gamma_5)u(p;\lambda_i), \quad (2)$$

where the $(i\gamma_5)$ multiplier ensures the correct P–parity properties of the considered amplitude, one can define the isoscalar amplitudes $\hat A$, $\hat B$, $\hat C$, $\hat D$ by

$$\hat M^{abc}_{\beta\alpha} = \hat A\tau^a_{\beta\alpha}\delta^{bc} + \hat B\tau^b_{\beta\alpha}\delta^{ac} + \hat C\tau^c_{\beta\alpha}\delta^{ab} + \hat D i\epsilon^{abc}\delta_{\beta\alpha}, \quad (3)$$

τ^a, $a = 1,2,3$ being the nucleon–isospin generators.

The analysis [12] of the spinor properties of the amplitude (2) allows to express each of isoscalar functions A, B, C, D in terms of 4 independent form factors in the following way

$$\begin{aligned}
\hat A &= S_A + \bar V_A\hat k + V_A\hat{\bar k} + i/2T_A[\hat k,\hat{\bar k}];\\
\hat B &= S_B + \bar V_B\hat k + V_B\hat{\bar k} + i/2T_B[\hat k,\hat{\bar k}];\\
\hat C &= S_C + \bar V_C\hat k + V_C\hat{\bar k} + i/2T_C[\hat k,\hat{\bar k}];\\
\hat D &= S_D + \bar V_D\hat k + V_D\hat{\bar k} + i/2T_D[\hat k,\hat{\bar k}]. \qquad (4)
\end{aligned}$$

Here, $k, \bar k$ are the crossing–covariant combinations of pion momenta

$$k = -k_1 + \epsilon k_2 + \bar\epsilon k_3; \quad \bar k = -k_1 + \bar\epsilon k_2 + \epsilon k_3, \quad (5)$$

where $\epsilon = \exp(2\pi i/3) = -1/2 + i\sqrt{3}/2$, $\bar\epsilon = \epsilon^* = -1/2 - i\sqrt{3}/2$. These combinations together with the independent crossing–invariant ones

$$Q \equiv -k_1 + k_2 + k_3 \;= p - q\;; \;\; P \equiv p + q \quad (6)$$

are used to define 5 independent scalar variables

$$\begin{aligned}
\tau = Q^2;\; \theta = Q\cdot k;\; \bar\theta = Q\cdot\bar k;\\
\nu = P\cdot k;\; \bar\nu = P\cdot\bar k, \qquad (7)
\end{aligned}$$

which completely determine the point in the phase space of the considered reaction. The expressions of all scalar products of particles' momenta are given in the paper [11] for the case of the unbroken isotopic symmetry. The definitions (5), (6), (7) are assumed for the physical particles. k_2 is the π^- momentum in the reactions $\{-+n\}$ $\{-0p\}$ and k_2 is the π^+ momentum in the reaction $\{+0p\}$. All actual kinematical calculations in the computer programs are processed with the isotopic symmetry breaking caused by the particles' masses; this complicates the expressions given in the quoted paper. For short we shall hold on the unbroken isotopic symmetry in the illustrations and in the discussions which follow.

The τ variable coincides with the squared mass of the virtual pion in the OPE graph. The 4π vertex of this graph is characterized also by the Mandelstam variables. The discussion of the off–shell dependence of the 4π vertex on these variables is given in the paper [13]. To avoid ambiguity we use only the dipion invariant mass

$$s_{\pi\pi} \equiv (k_2 + k_3)^2 \quad (8)$$

in the discussion below.

The amplitudes of the observable channels of the reactions $\pi N \to \pi\pi N$ with the convention for the normalization of the particle states adopted in [11] are provided by relations:

$$\begin{aligned}
&\hat M_{\{-+n\}} = \sqrt{2}/2(\hat A + \hat C);\;\; \hat M_{\{00n\}} = \;1/2(\hat A);\\
&\hat M_{\{++n\}} = 1/2(\hat B + \hat C);\;\; \hat M_{\{-0p\}} = \;1/2(\hat C - 2\hat D);\\
&\hat M_{\{+0p\}} = 1/2(\hat C + 2\hat D). \qquad (9)
\end{aligned}$$

The nontrivial statistical factors are taken into account for $\{0\,0\,n\}$ and $\{+\,+\,n\}$ channels.

These amplitudes have the same form as in (4)

$$\hat{M}_X = S_X + \bar{V}_X\hat{k} + V_X\hat{\bar{k}} + i/2T_X[\hat{k},\hat{\bar{k}}];$$
$$X = (\{-+n\},\{-0p\},\{00n\},\{++n\},\{+0p\}), \quad (10)$$

where the spinor structures are defined according to the expansions (9), e.g. $S_{\{-+n\}} = \sqrt{2}/2(S_A + S_C)$, etc. In practice, the following combinations of the vector form factors of decompositions (4), (10)

$$V_X^R \equiv (V_X + \bar{V}_X)/2; \;\; V_X^I \equiv (V_X - \bar{V}_X)/(2i) \quad (11)$$

are used in the course of calculations.

2.1.2 Cross section

The experimental data of the channel X are compared with the theoretical cross sections $\sigma^{\rm Th}_{(\alpha)}$ for a given experimental point (α)

$$\sigma^{\rm Th}_{(\alpha)} = \frac{\sigma_c}{4J}\int \frac{d^3k_2}{(2\pi)^3 2k_{20}}\frac{d^3k_3}{(2\pi)^3 2k_{30}}\frac{d^3q}{(2\pi)^3 2q_0} \times (2\pi)^4\delta^4(p+k_1-q-k_2-k_3)||M||^2\Theta_\alpha\,. \quad (12)$$

Here, $\sigma_c \equiv (\hbar c)^2 = 0.38937966(23)[\mathrm{GeV}^2\,\mathrm{mbn}]$ is the conversion constant,

$$4J = 4\sqrt{(p\cdot k_1)^2 - m_p^2\mu_1^2}$$

stands for normalization of the initial state and the characteristic function $\Theta_{(\alpha)} = \Theta_{(\alpha)}(p,k_1,\,q,k_2,k_3)$ of the bin (α) describes the appropriate cuts in the phase space if any; this function is equal to 1 for a total cross section. The notation $||M||^2$ is used for the squared modulus of the amplitude summed over polarizations of the final nucleon and averaged over ones of the initial proton. We shall call it simply *matrix element*. The statistical factor equal to the product of $1/n_\nu!$ over subsets of identical particles for calculation of the cross section was included into definitions (9) of the physical reaction amplitudes.

The matrix element $||M||^2 \equiv ||M_X||^2$ is the quadratic form of the vector of spinor structures $(S_X, V_X, \bar{V}_X, T_X)$ or, the same, of the vector (S_X, V_X^R, V_X^I, T_X):

$$\|M_X\|^2 \equiv 1/2\sum_{\lambda_f,\lambda_i}\left[\bar{u}(q;\lambda_f)\hat{M}_X(i\gamma_5)u(p;\lambda_i)\right] \times \left[\bar{u}(q;\lambda_f)\hat{M}_X(i\gamma_5)u(p;\lambda_i)\right]^* = \begin{pmatrix} S_X \\ V_X \\ \bar{V}_X \\ T_X \end{pmatrix}^\dagger G \begin{pmatrix} S_X \\ V_X \\ \bar{V}_X \\ T_X \end{pmatrix}, \quad (13)$$
$$(X = \{-+n\},\{-0p\},\{00n\},\{++n\},\{+0p\});$$

$$G \equiv \frac{1}{2}\mathrm{Sp}\left[(\hat{q}+m)\begin{Bmatrix} \hat{1} \\ \hat{k} \\ \hat{\bar{k}} \\ \frac{i}{2}[\hat{k},\hat{\bar{k}}] \end{Bmatrix}(\hat{p}-m)\gamma_0\begin{Bmatrix} \hat{1} \\ \hat{k} \\ \hat{\bar{k}} \\ \frac{i}{2}[\hat{k},\hat{\bar{k}}] \end{Bmatrix}^\dagger\gamma_0\right]. \quad (14)$$

The matrix G of the above form is given in the paper [11] for the simplified case of equal pion masses. In practice, the matrix for every channel had been calculated separately with the physical masses of all particles in the considered channel.

To plot the data and the theoretical results we define the "quasi–amplitude" $\langle M\rangle_{(\alpha)}$, which is the square root of the cross section (12), divided by the phase space $\sigma^{psv}_{(\alpha)} \equiv \sigma_{(\alpha)}(1)$:

$$\langle M\rangle_{(\alpha)} \equiv \sqrt{\frac{\sigma_{(\alpha)}(\|M\|^2)}{\sigma_{(\alpha)}(1)}}. \quad (15)$$

Here, the phase space $\sigma(1)$ is the theoretical cross section (12), calculated with the unit matrix element. In this manner we treat the total cross sections. In the case of distributions both the cross section and the phase space are independently normalized to 1 — we call this quantity *normalized* quasi–amplitude $\langle M_{(\alpha)}\rangle_{\rm norm}$:

$$\langle M_{(\alpha)}\rangle_{\rm norm} \equiv \sqrt{\frac{\sigma^n_{(\alpha)}(\|M\|^2)}{\sigma^n_{(\alpha)}(1)}}. \quad (16)$$

2.1.3 Remarks on sign ambiguity

To resume the discussion of the general structure of the $\pi 2\pi$ amplitude let us consider briefly the problem of the sign ambiguity in the theoretical amplitude which is used to fit the experimental cross section data. This ambiguity is already present at the threshold since the threshold limits of observable quasi–amplitudes are determined by two independent values of isotopic threshold amplitudes A^0 and B^0. Apart the overall sign ambiguity of isotopic threshold amplitudes their relative sign might also become indefinite depending on the accuracy of the experimental information.

In what follows we call the solution *physical* (*unphysical*) when A^0 and B^0 are of different (equal) signs. In terms of the $\pi\pi$–scattering lengths the two cases of signs correspond to the different (equal) signs of $a_0^{I=0}$ and $a_0^{I=2}$.

There are no simplifications at a distance from the threshold. Indeed, the expression (14) for the matrix element $\|M_X\|^2$ might be brought to the diagonal form, for example, in terms of the analogues of the diagonal derivative amplitudes of Rebbi [14], in which it becomes the sum of four squared modules of the orthogonal amplitudes. The abundance of solutions found in the course of data fittings should be explained in part by a variety of choices of signs of the above four orthogonal amplitudes in every channel.

2.2 Near–threshold $\pi N \to \pi\pi N$ phenomenology guidelines

We need to collect the basic known facts about the $\pi N \to \pi\pi N$ phenomenology in order to obtain the motivation for developing the model amplitude. This will be done in short.

1. The current knowledge of physics of the pion–nucleon interactions provides no evidence of possible mechanisms or processes resulting in the strong variation of the amplitude of the $\pi N \to \pi\pi N$ reaction in the phase space at energies up to $\approx 2m_\pi$ above threshold. All resonances but $N^{(*)}$ and Δ are located outside the phase space.

2. The contribution of the near–threshold Δ pole is only due to the chain $\pi N \to \Delta \to \pi\pi N$. It is suppressed 1) by the negligible width of the decay $\Delta \to \pi\pi N$ described by the $\pi\pi N\Delta$ vertex because of the vanishing phase space; 2) by Quantum mechanics: Δ is located precisely at the $\pi 2\pi$ threshold where the process $\pi N \to \pi\pi N$ must proceed through the waves P_{11} and P_{31} of the initial pion–nucleon system (in the L_{2I2J} notation) while Δ can be created only in the P_{33} wave of the π–N system. However, the same $\pi\pi N\Delta$ vertex gives rise to the crossing–related process $\pi N \to \pi\Delta \to \pi\pi N$ in which the Δ pole approaches the phase space at energies starting from $P_{\rm Lab} = 500$ MeV/c.

3. The threshold of $N^{(*)}$ creation in the initial state is located at $P_{\rm Lab} = 660$ MeV/c. Due to the width $\sim 170 \pm 50$ MeV the $N^{(*)}$ contribution must be nonnegligible up to the reaction threshold.

4. The contribution of the meson–resonance type closest to the phase space is that of OPE — all the other are very distant at the discussed energies.

5. The tails of resonances result in some constant background in the physical domain and, at most, in some slow variation of the amplitude. One would need the extraordinary precision of experimental data to distinguish between a linear function in the corresponding variable and the far pole.

6. The number of free or, unknown parameters in $\pi\pi$, πN, $\pi\Delta$, $\pi N^{(*)}$ interactions exceeds the number of degrees of freedom of the amplitude which is linear in the invariant independent variables.

7. All resonances contribute with terms built of various scalar products of momenta. There are at most five such products which might be considered to be independent or, the same, they are built of five invariant variables. Hence, an arbitrary linear function is parametrized with 6 parameters: a constant plus 5 coefficients at the variables. This applies to all form factors of 4 independent isospin amplitudes which describe 5 observable channels of the reaction.

8. There are four different spinor structures in the $\pi 2\pi$ amplitude. They provide the specific dependence on variables which might well be nonnegligent at some distance from the threshold even in the unpolarized experiment.

9. The Bose statistics, the isospin symmetry, the C–invariance and the crossing, being the exact properties of an amplitude derived according to the rules of quantum field theory, restrict the form of amplitude dependence on variables, making some parameters vanish and linking the rest parameters.

10. As a result there might be about 20 parameters for the near–threshold description of all channels and, in particular, no more than 15 for the $\pi^- p \to \pi^-\pi^+ n$ process. By the unitarity conditions which relate the nonvanishing $\pi 2\pi$ isospin amplitudes only with the P_{31} and P_{11} waves of elastic πN amplitudes, the above parameters must be approximately real. Only few of 20 imaginary parts of the polynomial background are expected to be of importance near the very threshold.

11. The discussed contributions must be combined with the explicit term describing the OPE amplitude and isobar contributions. This will provide about 20 additional parameters if D waves of the $\pi\pi$ scattering and all structures of the vertices $\pi\pi N\Delta$, $\pi\pi N^{(*)}\Delta$, $\pi\pi N N^{(*)}$ are important.

11. The cuts due to thresholds of another inelastic processes like the 3π production, the η production, etc. are conspired by nearby isobars.

12. The analysis of the paper [15] makes it evident that isobar resonances saturate the existing data on total cross sections below 1 GeV. Therefore, the imaginary part of the $\pi 2\pi$ amplitude might be described by the Breit–Wigner form of isobar contributions and the discussed above parameters of the imaginary background might appear to be negligible.

2.3 Resonance contributions to $\pi N \to \pi\pi N$ amplitude

The $\pi 2\pi$ amplitude to be developed must cover the energy interval from the threshold to the isobar region. Therefore, the approach of Oset–Vicente is the most suitable one for the discussed purpose since it admits the due account of isobar physics and can provide the maximal model independence of the obtained results. The keystone of our model is the account of all resonance mechanisms such that their contributions to the $\pi 2\pi$ amplitude provide a pole located either directly in the reaction phase space or in about a one–width distance from it at energies from the threshold to $P_{\rm Lab} \approx 500$ MeV/c.

Let us first enumerate the resonance–exchange graphs which are proper to our reaction, using the names of two–particle channels for labels. Three representatives $\mathrm{SE}_{\pi N}$, $\mathrm{SE}_{\pi\pi}$, SE_{NN} of inequivalent crossing–related single–pole graphs are shown in Fig. 1. Every four–particle vertex of the above graphs can be expanded in two different ways providing no more than three types of inequivalent double-pole graphs which we mark in $\mathrm{DE}_{\pi N,\pi N}$, $\mathrm{DE}_{\pi N,\pi\pi}$, $\mathrm{DE}_{NN,\pi\pi}$ (see Fig. 1). In what follows we shall use the self–explanatory notations like $\mathrm{SE}_{\pi N}\{\Delta\}$, $\mathrm{DE}_{NN,\pi\pi}\{\omega,\rho\}$ when discussing contributions of classes of crossing–related graphs. It is evident that all distinct resonances and particles responsible for pole contributions to the amplitude enter already the single–pole scheme; the particles which might be relevant to the intermediate energy amplitude are listed in Table 1. There are enough representatives of the lowest spin–isospin states in the lists $\mathrm{SE}_{\pi\pi}$, SE_{NN}. The list is far from being complete in the $\mathrm{SE}_{\pi N}$ channel. In the present paper we limited the contributions, taking into account the particles N, Δ, $N^{(*)}$, σ, ρ, π, ω and A; in fact, the interactions of σ, ω and A given below in the lists of lagrangians for the purpose of the forthcoming discussion were omitted from the actual analysis.

Table 1. Resonances and particles from PDG–96 [16] responsible for pole contributions to the low energy $\pi N \to \pi\pi N$ amplitude

$\mathrm{SE}_{\pi N}$	$I(J^P)$	$\mathrm{SE}_{\pi\pi}$	$I^G(J^{PC_n})$	SE_{NN}	$I^G(J^{PC_n})$
$N=(p,n)$	$\frac{1}{2}(\frac{1}{2}^+)$	$\sigma = f_0(400{-}1200)$	$0^+(0^{++})$	$\pi = (\pi^\pm, \pi^0)$	$1^-(0^{-+})$
$\Delta = \Delta(1232)$	$\frac{3}{2}(\frac{3}{2}^+)$	$\rho = \rho(770)$	$1^+(1^{--})$	$\omega = \omega(782)$	$0^-(1^{--})$
$N^{(*)} = N(1440)$	$\frac{1}{2}(\frac{1}{2}^+)$	$f = f_2(1270)$	$0^+(2^{++})$	$A = a_1(1260)$	$1^-(1^{++})$
$N' = N(1520)$	$\frac{1}{2}(\frac{3}{2}^-)$	$\rho' = \rho(1450)$	$1^+(1^{--})$	$\pi' = \pi(1300)$	$1^-(0^{-+})$
$\not{N} = N(1535)$	$\frac{1}{2}(\frac{1}{2}^-)$	$\cdots$		$\cdots$	
$\cdots$					

Table 2. Lagrangians for 4–particle vertices of the SE graphs

Graph [Vertex]	Lagrangian
$\mathrm{SE}_{\pi N}\{N\}$ $[\pi\pi NN]$	$g^1_{\pi\pi NN}\bar{N}\delta_{ab}N\pi^a\pi^b + g^2_{\pi\pi NN}\bar{N}\delta_{ab}N\partial^\mu\pi^a\partial_\mu\pi^b$ $+g^3_{\pi\pi NN}\bar{N}i\epsilon_{abc}\tau^c\gamma_\mu N[\partial^\mu\pi^a\pi^b - \pi^a\partial^\mu\pi^b]$ $+g^4_{\pi\pi NN}\bar{N}i\epsilon_{abc}\tau^c[\gamma_\mu,\gamma_\nu]N\partial^\mu\pi^a\partial^\nu\pi^b$
$\mathrm{SE}_{\pi N}\{N^{(*)}\}$ $[\pi\pi NN^{(*)}]$	$g^1_{\pi\pi NN^{(*)}}\bar{N}\delta_{ab}N^{(*)}\pi^a\pi^b + g^2_{\pi\pi NN^{(*)}}\bar{N}\delta_{ab}N^{(*)}\partial^\mu\pi^a\partial_\mu\pi^b$ $+g^3_{\pi\pi NN^{(*)}}\bar{N}i\epsilon_{abc}\tau^c\gamma_\mu N^{(*)}[\partial^\mu\pi^a\pi^b - \pi^a\partial^\mu\pi^b]$ $+g^4_{\pi\pi NN^{(*)}}\bar{N}i\epsilon_{abc}\tau^c[\gamma_\mu,\gamma_\nu]N^{(*)}\partial^\mu\pi^a\partial^\nu\pi^b + \{\mathrm{H.C.}\}$
$\mathrm{SE}_{\pi N}\{\Delta\}$ $[\pi\pi N\Delta]$	$\bar{N}(g^1_{\pi\pi N\Delta}F^0_{dbc} + 3g^2_{\pi\pi N\Delta}F^1_{dbc})i\gamma_5\Delta^d_\mu\partial^\mu\pi^b\pi^c$ $+\bar{N}(g^3_{\pi\pi N\Delta}F^0_{dbc} + 3g^4_{\pi\pi N\Delta}F^1_{dbc})\gamma_\nu\gamma_5\Delta^d_\mu\partial^\mu\pi^b\partial^\nu\pi^c + \{\mathrm{H.C.}\};$ $F^0_{dbc} = i\epsilon_{dbc} + \delta_{db}\tau_c - \delta_{dc}\tau_b; \quad F^1_{dbc} = \delta_{db}\tau_c + \delta_{dc}\tau_b - 2/3\ \delta_{bc}\tau_d$
$\mathrm{SE}_{NN}\{\pi\}$ $[\pi\pi\pi\pi]$	$V_{4\pi}$
$\mathrm{SE}_{NN}\{\omega\}$ $[\pi\pi\pi\omega]$	$g_{\pi\pi\pi\omega}\omega_\mu\partial_\nu\pi^a\partial_\alpha\pi^b\partial_\beta\pi^c i\epsilon_{abc}i\epsilon^{\mu\nu\alpha\beta}$
$\mathrm{SE}_{NN}\{A\}$ $[\pi\pi\pi A]$	$g^1_{\pi\pi\pi A}A^\mu_b\pi^b\pi^a\partial_\mu\pi^a$ $+g^2_{\pi\pi\pi A}A^\mu_b\partial_\mu\pi^b\partial_\nu\pi^a\partial^\nu\pi^a + g^3_{\pi\pi\pi A}A^\mu_b\partial_\nu\pi^b\partial_\mu\pi^a\partial^\nu\pi^a$
$\mathrm{SE}_{\pi\pi}\{\sigma\}$ $[\pi\sigma NN]$	$g_{\pi\sigma NN}\bar{N}\tau^a\gamma_\mu\gamma_5 N\partial^\mu\pi_a\sigma$
$\mathrm{SE}_{\pi\pi}\{\rho\}$ $[\pi\rho NN]$	$g^1_{\pi\rho NN}\bar{N}\gamma_\mu\gamma_\nu\gamma_5 N(\partial^\mu\pi_a\rho^\nu_a - \partial^\nu\pi_a\rho^\mu_a)/2$ $+g^2_{\pi\rho NN}\bar{N}\tau^a\gamma_5 N\partial_\mu\pi_b\rho^\mu_c i\epsilon_{abc}$

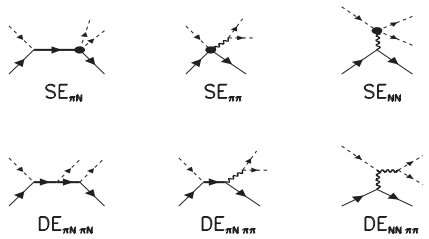

Fig. 1. Representatives of graphs of resonance contributions

Apart the OPE contribution our model is described by the effective interaction lagrangian which is used to construct the tree–level amplitude; all terms of the lagrangian are collected in Tables 2, 3. In general, we are trying to use the minimal derivative coupling especially when particles of the nontrivial spin, for example, in the $\rho N\Delta$ vertex, are being involved. Otherwise the terms of very high order in the momentum inevitably are present in the amplitude. However, when three–particle vertices contain the pion, like πNN, $\pi N\Delta$, etc., the vertices are brought to the derivative–coupling form. Having in mind the complete equivalence of nonderivative and derivative couplings in such vertices since in the difference of the corresponding amplitudes the propagators always become contracted, we assume that only other types of vertices, for example, 4π, $\pi\pi NN$, etc. are responsible for the explicit breaking of Chiral Symmetry.

Even in the brief summary of properties of the considered interactions we must point that the form of the four–particle vertices is chosen to represent all spin–isospin structures of the given vertex. This makes impossible to

Table 3. Lagrangians for 3–particle vertices of the DE graphs

Graph [Vertex]	Lagrangian
$\mathrm{DE}_{\pi N,\pi N}\{N,N\}$ $[\pi NN]$	$g_{\pi NN}\bar{N}\tau_a\gamma_\mu\gamma_5 N\partial^\mu\pi^a$
$\mathrm{DE}_{\pi N,\pi N}\{N,N^{(*)}\}$ $[\pi NN^{(*)}]$	$g_{\pi NN^{(*)}}\bar{N}\tau_a\gamma_\mu\gamma_5 N^{(*)}\partial^\mu\pi^a + \{\mathrm{H.C.}\}$
$\mathrm{DE}_{\pi N,\pi N}\{N,\Delta\}$ $[\pi N\Delta]$	$g_{\pi N\Delta}(\bar{\Delta}^a_\mu P_{ab} N\partial^\mu\pi^b + \bar{N}P^\dagger_{ab}\Delta^a_\mu\partial^\mu\pi^b)$
$\mathrm{DE}_{\pi N,\pi N}\{N^{(*)},N^{(*)}\}$ $[\pi N^{(*)}N^{(*)}]$	$g_{\pi N^{(*)}N^{(*)}}\bar{N^{(*)}}\tau_a\gamma_\mu\gamma_5 N^{(*)}\partial^\mu\pi^a$
$\mathrm{DE}_{\pi N,\pi N}\{N^{(*)},\Delta\}$ $[\pi N^{(*)}\Delta]$	$g_{\pi N^{(*)}\Delta}(\bar{\Delta}^a_\mu P_{ab} N^{(*)}\partial^\mu\pi^b + \bar{N^{(*)}}P^\dagger_{ab}\Delta^a_\mu\partial^\mu\pi^b)$
$\mathrm{DE}_{\pi N,\pi N}\{\Delta,\Delta\}$ $[\pi\Delta\Delta]$	$g_{\pi\Delta\Delta}\bar{\Delta}^a_\mu\gamma_\nu\gamma_5 A_{abc}\bar{\Delta}^b_\mu\partial^\nu\pi^c$, $A_{abc} = \frac{4}{9}(-2\delta_{bc}\tau_a - 2\delta_{ac}\tau_b + 8\delta_{ab}\tau_c - 5i\epsilon_{abc})$
$\mathrm{DE}_{\pi N,\pi\pi}\{N,\sigma\}$ $[\sigma NN]$	$g_{\sigma NN}\bar{N}N\sigma$
$\mathrm{DE}_{\pi N,\pi\pi}\{N,\rho\}$ $[\rho NN]$	$g^{\mathrm{V}}_{\rho NN}\bar{N}\gamma_\mu\tau^a N\rho^\mu_a + g^{\mathrm{T}}_{\rho NN}\bar{N}\sigma_{\mu\nu}\tau^a N\partial^\mu\rho^\nu$
$\mathrm{DE}_{\pi N,\pi\pi}\{N^{(*)},\sigma\}$ $[\sigma NN^{(*)}]$	$g_{\sigma NN^{(*)}}\bar{N}N^{(*)}\sigma + \{\mathrm{H.C.}\}$
$\mathrm{DE}_{\pi N,\pi\pi}\{N^{(*)},\rho\}$ $[\rho NN^{(*)}]$	$g^{\mathrm{V}}_{\rho NN^{(*)}}\bar{N}\gamma_\mu\tau^a N^{(*)}\rho^\mu_a + g^{\mathrm{T}}_{\rho NN^{(*)}}\bar{N}\sigma_{\mu\nu}\tau^a N^{(*)}\partial^\mu\rho^\nu + \{\mathrm{H.C.}\}$
$\mathrm{DE}_{\pi N,\pi\pi}\{\Delta,\rho\}$ $[\rho N\Delta]$	$g_{\rho N\Delta}\bar{\Delta}^a_\mu P_{ab} N\rho^{\mu b} + \{\mathrm{H.C.}\}$
$\mathrm{DE}_{NN,\pi\pi}\{\pi,\sigma\}$ $[\pi\pi\sigma]$	$g_{\pi\pi\sigma}\sigma\partial_\mu\pi^a\partial^\mu\pi^a$
$\mathrm{DE}_{NN,\pi\pi}\{\pi,\rho\}$ $[\pi\pi\rho]$	$g_{\pi\pi\rho}\partial^\nu\rho^\mu_a\partial_\nu\pi^b\partial_\mu\pi^c\epsilon_{abc}$
$\mathrm{DE}_{NN,\pi\pi}\{\omega,\rho\}$ $[\pi\rho\omega]$	$g_{\pi\rho\omega}\omega_\mu\partial_\nu\pi^a\partial_\alpha\rho^a_\beta i\epsilon^{\mu\nu\alpha\beta}$
$[\omega NN]$	$g^{\mathrm{V}}_{\omega NN}\bar{N}\gamma_\mu N\omega^\mu + g^{\mathrm{T}}_{\omega NN}\bar{N}\sigma_{\mu\nu}N\partial^\mu\omega^\nu$
$\mathrm{DE}_{NN,\pi\pi}\{A,\sigma\}$ $[\pi\sigma A]$	$g_{\pi\sigma A}A^\mu_a\partial_\mu\pi^a\sigma$
$\mathrm{DE}_{NN,\pi\pi}\{A,\rho\}$ $[\pi\rho A]$	$[g^1_{\pi\rho A}\partial^\mu\pi^a\partial_{[\mu}\rho^b_{\nu]}A^{\nu c} + g^2_{\pi\rho A}\partial^\mu\pi^a\rho^{\nu b}\partial_{[\mu}A^c_{\nu]}]i\epsilon_{abc}$
$[ANN]$	$g^{\mathrm{V}}_{ANN}\bar{N}\gamma_\mu\gamma_5\tau^a N A^\mu_a + g^{\mathrm{T}}_{ANN}\bar{N}\sigma_{\mu\nu}\gamma_5\tau^a N\partial^\mu A^\nu$

fix the lagrangian parameters from the decay data. For example, the known width for $N^{(*)} \to \pi\pi N$ provides only bounds for 4 parameters of the $\pi\pi NN^{(*)}$ lagrangian given in the Table 2. However, we prefer to avoid any doubt in respect to a possible model dependence of the results for $\pi\pi$–scattering lengths or, at least, to leave a chance for checking the presence of such dependence.

We are using the simplest form

$$S^{\mu'\mu}_M(k) = \frac{1}{3M^2}\Big[-3M^2 g^{\mu'\mu} + M^2\gamma^{\mu'}\gamma^\mu + 2k^{\mu'}k^\mu - M(k^{\mu'}\gamma^\mu - \gamma^{\mu'}k^\mu)\Big] \quad (17)$$

for the nominator of the propagator of a $(3^+/2)$ particle. The $iM\Gamma$ shifts regularizing the terms with poles located in the physical region, were made also for all cross terms to ensure correct crossing properties of the entire amplitude.

The central contribution to our amplitude is supposed to come from the OPE graph $\mathrm{SE}_{NN}(\pi)$. It is parametrized with the use of the cross–symmetric threshold expansion of the 4π vertex elaborated in the paper [17]. Apart the account of the imaginary part the expansion in the $O(k^4)$ order is equivalent to the form described in the papers [12, 11]. The results of the present work which will be discussed below confirm that the precision of the currently available experimental data does not allow to consider higher terms of the $\pi\pi$ amplitude.

We list the interactions most part of which had been used for the construction of the phenomenological ampli-

tude, entering the data fittings, in Tables 2, 3 below. Since all 3–particle vertices of the SE series of graphs are present also in the DE graphs we do not describe them separately — see Table 3. The symbol $V_{4\pi}$ stands for the $\pi\pi$ interaction in Table 2; this contribution is taken in the direct amplitude form.

The listed lagrangians and the Feynman rules of the tree approximation determine the resonance part of our amplitude. The contributions generally come to all 16 scalar–isoscalar form factors defined in (3), (4). Unfortunately, it is impossible to present the final answers in somehow short terms. The reason stems from the large number of cross terms provided by Feynman rules. Such terms are distinct for every form factor and their number might be equal to 12, 6 and 3. The last value corresponds to the OPE diagram. The number equals 12 for almost all the rest diagrams.

2.4 Background contribution to $\pi N \to \pi\pi N$ amplitude

An important issue of the approach [12,11] developed for the near–threshold energy region is given by the linear background terms presented in the form such that it respects the symmetries of strong interactions, namely, P, C, T, $SU_F(2)$ and crossing. To modify this ingredient of the model we need to discuss the role of these smooth terms in the amplitude.

Initially, such terms were added to the OPE ones to stand for all other possible mechanisms of the $\pi N \to \pi\pi N$ reaction. When taking into account only a part of contributions of particles listed in Table 1 one leaves enough room for the background terms standing for the rest resonances.

Another reason for the presence of a background is connected with ambiguities which are specific to the off–shell interactions of high–spin particles (see, for example, the old discussion [18–20]). These interactions result in polynomial terms in the considered amplitude and polynomial terms in the 4–particle vertices. The overall contribution of this kind coming from all resonances is constrained by the asymptotic conditions for the entire amplitude. In principle, this makes necessary to use the consistent theory for particle propagators and all vertices like πNN, $\pi N\Delta$, etc. Leaving the parameters of the polynomial background free we are safe to use the propagators and the vertices in the form determined by the simplicity reasons and/or by the chiral–symmetry arguments.

Since we are regularizing the exchange graphs which have poles in the physical region by the $iM\Gamma$ shift in the propagators, the polynomial background must have both real and imaginary parts.

The discussed nature of the background terms forces us to modify the model of the papers [12,11] in two directions. First, we add the second order terms in variables (7) to the scalar structures S_A, S_B, S_C, S_D. This makes the dimensions of the tensor and the scalar structures of the decomposition (4) be balanced. The final form of the background amplitude becomes

$$
\begin{aligned}
S_A &\equiv S_A(\tau,\nu,\bar\nu,\theta,\bar\theta) = A_1 + A_2\tau + A_3(\theta+\bar\theta) \\
&\quad + A_{12}\tau^2 + A_{13}\bar\nu\nu + A_{14}\bar\theta\theta + A_{15}(\nu^2+\bar\nu^2) \\
&\quad + A_{16}(\theta^2+\bar\theta^2) + A_{17}\tau(\theta+\bar\theta)\,; \\
S_B &= S_A(\tau,\bar\epsilon\nu,\epsilon\bar\nu,\bar\epsilon\theta,\epsilon\bar\theta)\,;\ S_C = \ S_A(\tau,\epsilon\nu,\bar\epsilon\bar\nu,\epsilon\theta,\bar\epsilon\bar\theta)\,; \\
S_D &= A_{18} i(\nu\bar\theta - \theta\bar\nu)\,; \qquad (18) \\
V_A &\equiv V_A(\tau,\nu,\bar\nu,\theta,\bar\theta) = A_4 + A_5\tau + A_6\theta + A_7\bar\theta\,; \\
V_D &= iA_9\nu\,; \\
V_B &= \epsilon V_A(\tau,\bar\epsilon\nu,\epsilon\bar\nu,\bar\epsilon\theta,\epsilon\bar\theta)\,;\ V_C = \ \bar\epsilon V_A(\tau,\epsilon\nu,\bar\epsilon\bar\nu,\epsilon\theta,\bar\epsilon\bar\theta)\,; \\
\bar V_A &= [V_A(\tau,\nu,\bar\nu,\theta,\bar\theta)]^*\,; \\
\bar V_B &= \bar\epsilon[V_A(\tau,\bar\epsilon\nu,\epsilon\bar\nu,\bar\epsilon\theta,\epsilon\bar\theta)]^*\,; \\
\bar V_C &= \epsilon[V_A(\tau,\epsilon\nu,\bar\epsilon\bar\nu,\epsilon\theta,\bar\epsilon\bar\theta)]^*\,; \\
\bar V_D &= -iA_9\bar\nu\,; \qquad (19) \\
T_A &\equiv T_A(\tau,\nu,\bar\nu,\theta,\bar\theta) = \ iA_8(\nu-\bar\nu)\,; \\
T_D &= A_{10} + A_{11}\tau\,; \\
T_B &= T_A(\tau,\bar\epsilon\nu,\epsilon\bar\nu,\bar\epsilon\theta,\epsilon\bar\theta)\,; \\
T_C &= T_A(\tau,\epsilon\nu,\bar\epsilon\bar\nu,\epsilon\theta,\bar\epsilon\bar\theta). \qquad (20)
\end{aligned}
$$

The use of the higher polynomial background requires to make calculations with about a hundred of the next order terms with free parameters or to find the reasons for rejecting most of them.

Second, becides 18 terms of the *real* background given by (18)–(20) we inserted the *imaginary* background into the amplitude. Its analitical form exactly reproduces the analitical form of the real background with its own distinct coefficients.

Let us now clarify the concept of *contribution* which we are widely using throughout the paper. From the point of view of Chiral Dynamics the usage of notions like the background contribution (a part of which the so called contact terms are), the contribution of OPE, etc. is meaningless since the field redefinition does not allow a separate graph to be well–defined — see the relevant discussion in the book [21]. The absence of the common solution on the role of the higher–spin baryons in ChPT makes the above notions even more ambiguous. Nevertheless, such quantities as the residues of the poles and the on–shell parameters of $V_{4\pi}$ are well–defined — these very quantities are in the focus of our project. As for the off–mass–shell contributions, in particular, the OPE one, we take them as they are, the Lagrangian source and Feynman rules providing the model–dependent answer. The field redefinition then modifies, first, the polynomial background terms and, second, the parameters of SE graphs. It has been already pointed out that we are leaving the background parameters free and keeping all spin–isospin structures of 4–particle vertices being represented — this helps to avoid the dependence of the results on a particular model.

To summarize, the considered amplitude contains 36 free parameters of the polynomial background, 4 free parameters of the real part of the OPE contribution and 5 formal parameters of its imaginary part (their relations with parameters of the real part are described in the paper [17]) and parameters from the lists of Table 2 and Table 3 discussed in the previous subsection. In the current paper we shall discuss the fittings performed with 21 parameters

from the above lists coming from the exchanges $\mathrm{SE}_{\pi N}(N)$, $\mathrm{SE}_{\pi N}(\Delta)$, $\mathrm{SE}_{\pi N}(N^{(*)})$, $\mathrm{SE}_{\pi\pi}(\rho)$, $\mathrm{DE}_{\pi N,\pi N}\{N,N\}$, $\mathrm{DE}_{\pi N,\pi N}\{N,\Delta\}$, $\mathrm{DE}_{\pi N,\pi N}\{N,N^{(*)}\}$, $\mathrm{DE}_{\pi N,\pi N}\{N^{(*)}, N^{(*)}\}$, $\mathrm{DE}_{\pi N,\pi N}\{N^{(*)}, \Delta\}$, $\mathrm{DE}_{\pi N,\pi N}\{\Delta,\Delta\}$ only.

3 Experimental base

The experimental base for fitting the amplitude parameters was built of the total cross sections in all five channels of the considered reaction in the energy region $P_{\mathrm{Lab}} \leq$ 500 MeV/c [22], [23], [24], [25], [26], [27], [28], [29], [30], [31], [32], [33], [34], [35], [36], [37], [38], [39], [40], [41], [42], [5], [43], [6], [46], [44], [45] and the distributions measured in the hydrogen bubble–chamber experiments at these energies [39,40,31,46,35]. The bubble–chamber data were preferred since they satisfy the condition of the coverage of the reaction phase space in the most complete way, the only restrictions being $P_{\mathrm{proton}} \geq 120$ MeV/c and $P_{\pi} \geq 30$ MeV/c which correspond to 5 mm of the flight distance. The losses occupy only a small part of the phase space namely, ≤ 2 % in the case of $\{\pi^-\pi^0 p\}$ and ≤ 3 % in the case of $\{\pi^-\pi^+ n\}$ at $P_{\mathrm{beam}} = 400$ MeV/c and might be easily taken into account during the calculations of theoretical distributions. Besides, the systematic errors of the bubble–chamber experiments are also minimal.

In the course of our fittings we faced the following problem. There are three works in the $\{\pi^-\pi^+ n\}$ channel at close beam momenta:

1. Kirz ($P_{\mathrm{Lab}} = 485$ MeV/c) [40],
2. Blokhintseva ($P_{\mathrm{Lab}} = 457$ MeV/c) [31],
3. Saxon ($P_{\mathrm{Lab}} = 456$ MeV/c) [46].

It was found that results of these works are incompatible. If one tries to describe only distributions from these works without appealing to any other data then the averaged χ^2 per bin ($\equiv \overline{\chi^2}_{p.b.}$) for distributions by Kirz and Blokhintseva separately and for their sum as well is less than 1. Adding the distributions by Saxon we obtained $\overline{\chi^2}_{p.b.} > 1.5$ for every combinations and even $\overline{\chi^2}_{p.b.} = 2.1$ for the Saxon's distributions themselves.

We should note here, that we have the results of the experiment by Blokhintseva as the collection of events. Hence, we can build any distribution and we did so for all kinds of distributions published in the Saxon's paper. Along with other spectra such distributions also represent the Blokhintseva work [31] in our fittings.

The experiment by Saxon contains more events than the ones by Kirz and Blokhintseva together, so, at first glance, one should prefer to choose his results. However, the processing of films had been performed by the Saxon's group in a quite specific nontraditional way. In such films the elastic $\{\pi^- p\}$ reaction events look very much like the events of the considered reaction, their total number being ten times greater. To economize manual measurements the group had estimated visually the density of the positive tracks and, basing on the estimate, had selected the events with π^+.

However, besides the velocity of the charged particle the density of a track in the bubble chamber depends upon much more another factors like the moment of particle flight relative to the moment of liquid expansion start, the moment of snapshot relative to the moment of particle flight, the liquid superheating degree, etc. This dependence is extremely strong. The above parameters undergo stabilization but the latter never becomes ideal. The rest fluctuations can not prevent the ionization measurements of tracks but for the reliability of the determination of the particle velocity in the every snapshot the control measurements of the bubble density should be performed for the sample track. The probability of an error is big in the visual estimating especially for the so large number of the processed tracks.

One can estimate the systematic error of the Saxon's work in the following way. The elastic events accidentally selected into the list of the considered reaction anyway will be rejected after measurements by the reaction fit results. The inelastic ones for which the positive track was erroneously identified as the proton one are lost forever. In such a way the statistics become more poor, the parts of the phase space for which the π^+ velocities are small suffering the most significant losses. The measured value of the total cross section is given in the Saxon's work as 1 mbn; since the results of all isotopic analyses of all set of total cross sections data provide the value of 1.4 mbn one can deduce the 30% level of losses of events in the "economizing" routine of the reaction analysis.

So large value of systematic error forced us to withdraw the distributions of the paper [46] from our fittings.

Thus, the distributions liable to treatment belong to three channels of the considered reaction: $\{\pi^-\pi^+ n\}$, $\{\pi^-\pi^0 p\}$, $\{\pi^+\pi^+ n\}$. The data on distributions of works [39], [40], [46], [35] were taken from the journal publications. The major part of distributions of the work [31] has never been published. These are the distributions in the following variables: the squares of invariant masses of all pairs of final particles $W_{\pi^-\pi^+}$, $W_{\pi^- n}$, $W_{\pi^+ n}$, the invariant variables τ, ν_R, ν_I, θ_R, θ_I introduced in [12,11], the cosine of the angle between the planes determined by CMS momenta of a) the beam and the recoil neutron; b) π^+ and π^- ($\cos\theta_{\pi\pi}$), the cosines of CMS angles of final particles with the beam $\cos\theta_{\pi^-}$, $\cos\theta_{\pi^+}$, $\cos\theta_n$, the angle $D\phi = \phi^- - \phi^+$ of the planes determined by CMS momenta of a) the beam and the π^- meson; b) the beam and the π^+ meson, the azimuth angle ϕ_{beam} and the cosine of the polar angle of the beam $\cos\theta_{\mathrm{beam}}$ in the Saxon reference frame in which the x axis is the direction of the neutron momentum, the z axis being along the vector product of the neutron momentum with the momentum of π^+ meson, $[\mathbf{p}_{\mathrm{n}}, \mathbf{p}_{\pi^+}]$.

The Jones paper (the $\{\pi^-\pi^+ n\}$ and $\{\pi^-\pi^0 p\}$ channels at $P_{\mathrm{Lab}} = 415$ MeV/c) [35] provides distributions in the squares of invariant masses of all pairs of final particles namely, $\{\pi^-\pi^+ n\}$: $W_{\pi^-\pi^+}$, $W_{\pi^- n}$, $W_{\pi^+ n}$; $\{\pi^-\pi^0 p\}$: $W_{\pi^-\pi^0}$, $W_{\pi^- p}$, $W_{\pi^0 p}$.

The Kirz paper (the $\{\pi^-\pi^+n\}$ channel at $P_{\rm Lab} = 485$ MeV/c) [40] gives distributions in the invariant masses $W_{\pi^-\pi^+}$, W_{π^-n}, W_{π^+n} of all pairs of final particles and in the cosine of angles of all final particles with the beam in CMS $\cos\theta_{\pi^-}$, $\cos\theta_{\pi^+}$, $\cos\theta_n$.

Another paper by Kirz (the $\{\pi^+\pi^+n\}$ channel at $P_{\rm Lab} = 477$ MeV/c) [39] contains distributions in the CMS angles of final particles θ_{π^+}, θ_n, the π^+ CMS energy $T_{\pi^+{\rm CMS}}$, the momentum P_{π^+} of π^+ in the (π^+,π^+) system and in the nonrelativistic momentum transfer $P_{\rm transf}$.

One should note that some of these distributions strongly differ from the distribution provided by the empty phase space while there are some with the insignificant difference. This becomes especially clear in terms of normalized quasi–amplitudes — see pictures in Figs. 3–8 where almost all distributions are reproduced.

We are using 94 points of the total cross sections data which were selected on the grounds of the compatibility analysis of the paper [47] from the total list of 105 experimental points.

There were used two experimental data points more in some variants of fittings namely, when the theoretical amplitude was not completely real — see the next section where all variants are described in more details. These points were fixing the phases of two isotopic amplitudes, nonvanishing at the threshold, by the known values of the elastic P_{31} ($\approx -4^\circ$) and P_{11} ($\approx 2^\circ$) phases in accordance with the final–state interaction theorem.

4 Data analysis

The analysis of the data described in the previous section required some preliminary steps which are described below. After then we discuss the main results in the Subsect. 4.2.

4.1 Principal steps of analysis

To perform the analysis the following steps had been done:

1. The contributions of every parameter of our model discussed in Sect. 2 to the amplitude had been calculated analytically according to the Feynman rules of the tree approximation. The expressions for all 16 scalar–isoscalar form factors defined in (3), (4) had been obtained and transformed to the FORTRAN code with the help of the REDUCE package [48] for analytic calculations in high energy physics.

2. The goal of the second step was the simplification of the data fitting routine for saving a lot of time during thousands of fitting iterations. For a given experimental point (α) the theoretical quantity $\sigma^{\rm Th}_{(\alpha)}$ confronting the experimental value $\sigma^{\rm Exp}_{(\alpha)}$ is the integral of the squared modulus of the amplitude (10) over the reaction phase space or, over its part in the case of the distribution data.

Since the set of all parameters $\{A_\nu\}$, including the formal ones, enters our amplitude linearly and the conditions for the formal parameters do not contain kinematics we can present the theoretical quantity (12) in the form

$$\sigma^{\rm Th}_{(\alpha)} = \sum_{\mu,\nu} A_\mu A_\nu C^{\mu\nu}_{(\alpha)}. \tag{21}$$

Then we can build for every experimental point (α) the *correlator* $C^{\mu\nu}_{(\alpha)}$ performing all phase space integrations ones and forever. These calculations had been done for every bin of all distributions with the use of the standard high energy physics package based on the Monte Carlo integration. Since all distributions in question belong to the beam momenta 415, 460, 477, 485 MeV/c few Monte Carlo runs were necessary and sufficient to provide the calculations. The correlator matrix $\hat{C}_{(\alpha)}$ for a total cross–section experimental point (α) was being recovered during the fittings' run–time by the fast interpolation from 13 fulcrum matrices in every channel precalculated at beam momenta 280, 285, 290, 300, 325, 350, 375, 400, 450, 500, 550, 600 and 650 MeV/c. The calculations of the fulcrum matrices had been performed with the fast and efficient program of Gauss integration described in the paper [49].

3. The content of the third step was the data fittings themselves. Here, we point only the general features and specifics of the approach; more details will be revealed along with the discussion of results.

The fittings had been performed by minimizing the value of χ^2 defined as

$$\chi^2 = \sum_{(\alpha)} \frac{(\sigma^{\rm Th}_{(\alpha)} - \sigma^{\rm Exp}_{(\alpha)})^2}{(\Delta\sigma^{\rm Exp}_{(\alpha)})^2} \tag{22}$$

for the total cross–section data. However, to avoid the artificial increase of the statistical weight of the total–cross–section data point for which the numerous distributions also were undergoing fittings we were using the distributions' data $\sigma^{\rm Exp}_{(\alpha)n}$ which were *normalized* to 1 instead of the total cross section.

The use of the precalculated correlator matrices $\hat{C}_{(\alpha)}$ and the simplicity of the expression (21), being calculated in the course of the iterative minimization of χ^2, made it possible to perform thousands of fitting runs each of which executing hundreds or even few thousands of iterations. The same specifics of the approach provided the excellent flexibility in respect to variation of both the set of fitting parameters and the set of experimental points. The numerous variants of fittings will be discussed in the next subsection.

4.2 Major results of analysis

Already test runs of fitting the distribution data had shown that the simple model of the paper [11] is unlikely to be capable to provide a satisfactory description. Therefore, the first question we were trying to find the answer to was if there exists a relatively simple model consistent with the selected data base of 411 experimental points. The answer was "no" and let us now discuss why.

We had been grouping together parameters related to one or another mechanism of the considered reaction since it ought to be a hard task to test $\approx 2^{61}$ variants of all combinations of parameters. There were 7 such groups in total, the largest ones consisting of the sets of the background parameters. Below we are using the following symbolic notations for these groups:

"b" — parameters of the real background;

"i" — parameters of the imaginary background;

"o" — parameters of the OPE contribution;

"r" — 3 parameters related to the ρ meson;

"N" — parameters of the nucleon contributions (namely, $\mathrm{SE}_{\pi N}\{N\}$ and $\mathrm{DE}_{\pi N,\pi N}\{N,N\}$ ones);

"D" — parameters of the Δ contributions (namely, $\mathrm{SE}_{\pi N}\{\Delta\}$, $\mathrm{DE}_{\pi N,\pi N}\{N,\Delta\}$ and $\mathrm{DE}_{\pi N,\pi N}\{\Delta,\Delta\}$ ones);

"R" — parameters of the $N^{(*)}$ contributions (namely, $\mathrm{SE}_{\pi N}\{N^{(*)}\}$, $\mathrm{DE}_{\pi N,\pi N}\{N,N^{(*)}\}$, $\mathrm{DE}_{\pi N,\pi N}\{N^{(*)},N^{(*)}\}$ and $\mathrm{DE}_{\pi N,\pi N}\{N^{(*)},\Delta\}$ ones).

For all possible combinations of the listed groups there had been performed the data fittings with at least 50 random starts. In general, no new solutions had been being revealed after 20–30 starts. When the number of distinct solutions was greater than usual we had been continuing the search with the increased number of random starts to 100 and more. With one exception this had not provided new solutions apart the solutions with incomparably large χ^2. Only in the "DRNbior" variant when all groups had been being involved acceptable distinct solutions had been found after 100 starts. The total list of this variant contains 11 solutions. It should be noted that the latter variant is the most difficult in fitting: the convergence is slow because of huge correlations between parameters, the parameter errors in the gained solutions being too large. Therefore, we consider the probability of existence of a missed solution to be negligible.

The values of χ^2 of the best solutions are listed in the Table 4. A part of solutions is withdrawn there to make the table more compact. The baryon–exchange mechanisms are combined with the sets of parameters "b", "i", "o" and "r". For example, the box in the "DR" row and "bio" column corresponds to "DRbio" variant, etc.; in the column (row) with the empty title we collect the results corresponding to the "pure" mechanism. Initially, the "r" set was considered as a *perturbation* to the basic amplitude since the relatively narrow ρ resonance might get into the reaction phase space at $P_{\mathrm{Lab}} \approx 800$ MeV/c only. However, the presented values of χ^2 can not provide the inference that the "r" mechanism is unimportant unless all baryon–exchange mechanisms are committed to action.

It is the examination of the Table 4 which leads to the following conclusions:

1. There is no particle for which a simple exchange mechanism is capable to describe the data.

2. Among the double–particle exchanges the participation of OPE does not look advantageous. Even the dummy "r" mechanism looks more preferable sometimes.

3. The leading order ChPT fails to describe the data. Indeed, all contact terms of Chiral Dynamics and tree–level graphs are contained in the variant "Nbo"; the result of the latter looks depressing even for free parameters.

4. The most significant improvement of χ^2 is achieved when the imaginary background "i" is being added; the participation of Δ and $N^{(*)}$ exchanges with the strong imaginary part of contributions is leading almost to the same effect.

To make the above general conclusions the knowledge of the absolute χ^2 values was sufficient, especially, since the number of experimental points considerably exceeds the number of free parameters. For a more subtle deduction one needs an information on χ^2_{DF} i.e. χ^2 per degree of freedom. However, before calculating χ^2_{DF} one first ought to look if there are undetermined and inessential parameters in the solution.

Now we must note the following feature of the discussed results. The numerous solutions in some variants reflect the existence of large correlations of parameters in the variant in question. The estimation of parameter errors by the fitting routine is not then precise enough and our simple algorithm for comparison of solutions marks as different the solutions which are, in principle, identical.

To make the situation clear and, what is more important, to reduce the errors of parameters we had performed the series of additional runs eliminating one by one that parameters the relative errors of which had been being greater than 1 and fitting the data by the rest parameters while the value of χ^2_{DF} had been improving. This routine had been applied to all solutions. Unfortunately, there is no enough room to display the results. The Table 5 presents the information on χ^2_{DF} for some selected variants, the number of parameters in effect N_{P} and the independent lowest $\pi\pi$ scattering lengths. The results of eliminating parameters had no influence on the above conclusions **1.**–**4.** whereas the number of parameters in effect had been considerably reduced. The new inferences derived from the Table 5 read:

5. The considered data base requires a complicated model for its description. Below the level of $\chi^2_{\mathrm{DF}} < 1.50$ the absolute minimum of the parameter number is 22 in the variant "Nbi"; for the most part of the acceptable solutions the number is greater than 30.

6. Assuming that the sequence of signs +, −, + of the $\pi\pi$ scattering lengths $a_0^{I=0}$, $a_0^{I=2}$, $a_1^{I=1}$ is *physical*, one finds that a half of all acceptable solutions with the OPE contribution falls to the *unphysical* sector. We remind that the physical sequence is the one which is consistent with predictions of Chiral Dynamics.

7. The results of fittings can not improve the precision of determinations of $\pi\pi$ scattering lengths. For example, the region $0.06 \le a_0^{I=0} \le 0.19$ might be derived from the Table 5 as the preferable one; however, even the current experimental value [50] $a_0^{I=0} = 0.26$ can not be rejected on the ground of the χ^2_{DF} criterion.

8. The predictions of ChPT in the next–to–leading order [51] $a_0^{I=0} = 0.20$, $a_0^{I=2} = -0.041$, $a_1^{I=1} = 0.036$, $a_2^{I=0} = 0.002$ are compatible with the data base; the separate fittings with the OPE parameters being kept fixed by the above values of scattering lengths, resulted in so-

Table 4. List of χ^2 in distinct solutions obtained from random start (50 tests) with $N_{\rm Exp} = 411$ experimental points. In the truncated variant "DRNbior" there are 12 solutions in total obtained in ≈ 500 runs

		o	b	bo	bi	bio	bir	bior
		8078.5	6993.9	6799.1	773.28	595.53	598.99	550.87
		9083.8	6996.4	6798.8	854.11	597.10	601.17	556.10
		12115.	6998.0	6800.8			620.91	563.68
			7016.9	6813.2			629.66	570.10
				6823.0				576.84
D	9936.3	987.7	634.49	622.43	546.35	517.90	527.54	491.08
		1105.3	651.55	634.08	546.52	520.18	531.11	493.17
			748.07	644.39	548.19		534.24	
				672.37			544.76	
R	6138.6	1160.2	746.19	618.26	511.88	499.41	468.06	453.23
		1378.3	756.55	636.47	515.07	505.34	484.49	502.90
		3988.6	761.74	638.38		566.52	517.41	523.12
				672.74				
				676.47				
N	13693.	7069.7	6660.6	6649.4	549.83	525.73	513.17	496.87
	13709.	7341.0	6660.8	6649.9	551.27	526.72	515.28	497.00
		7388.9	6668.7	6653.0		527.84	516.82	498.42
		9928.6	6739.4	6674.7		528.84	518.16	500.98
			8508.0	6707.2			518.89	501.18
				6731.2				
D	2758.5	760.88	578.68	564.35	471.09	469.33	448.73	443.09
R		870.24	586.21	566.70	475.71	469.96	466.93	450.85
		978.58	659.71	568.58	483.21	470.86	469.82	
		3544.5		573.63	494.95	479.92	473.89	
						482.53		
D	4438.7	647.74	557.32	550.95	495.19	485.30	473.29	444.11
N	5023.7	793.23	562.20	555.25	496.55	487.58	481.65	463.69
			572.59	561.61	513.20		496.34	
			619.67	574.84				
				576.49				
				609.92				
R	2546.7	907.85	553.01	540.30	467.26	455.12	442.69	426.66
N		1067.6	553.04	568.76	499.38	487.41	486.08	480.20
		2997.9	553.21		519.16	493.38		
			555.16					
			584.36					
D	1430.1	588.65	510.42	506.13	435.72	430.88	426.54	412.84
R	1430.7	710.41	516.79	507.26	449.27	442.20	432.59	418.83
N	1451.5				449.62	443.02	435.85	423.30
					450.10	445.69	447.12	589.75
								******

lutions with the values of $\chi^2_{\rm DF}$ very close to the best ones; for example, in the "DRNbior" variant we get $\chi^2_{\rm DF}$ in the range 1.175 — 1.200.

9. The formal parameters of the imaginary part of the OPE contribution are insignificant at the considered energy region. This is the result of the separate investigations; eliminating these parameters we get some shifts in the parameters of the imaginary background and in the parameters of $N^{(*)}$ and Δ isobars, the real parameters of OPE remaining the same.

10. The discussed above routine of eliminating parameters provided further support of the point **5.**: no one of the considered mechanisms had been rejected as a whole in the course of improving the $\chi^2_{\rm DF}$ value.

The listings of this routine contain also a large volume of information about the significance of a given parameter in terms of the "statistical" frequency of its participation. For example, in all variants the parameters A_2, A_3 and A_4 of the linear background of [11] and the parameters A_{13} and A_{15} of (18) were found to be necessary whereas the parameter A_{11} entering the tensor structure of the amplitude $\hat{D}$ given by (20) had been always ignored. In respect to the OPE parameters the content of the Tables 5, 4 already shows that the parameters are not of the top significance since there are many acceptable solutions without the OPE contribution at all. The parameter g_1 of the paper [11] is found to be relatively important, the D–waves parameters g_2, g_3 being much less necessary.

Table 5. List of $\chi^2_{\rm DF}$ in distinct solutions obtained after deleting undetermined parameters; $N_{\rm Exp} = 411$ experimental points. To save the space only the best *unphysical* solutions of the "DRNbior" variant are shown

	bi		bio					bir		bior				
	$\chi^2_{\rm DF}$	$N_{\rm P}$	$\chi^2_{\rm DF}$	$N_{\rm P}$	$a_0^{I=0}$	$a_0^{I=2}$	$a_1^{I=1}$	$\chi^2_{\rm DF}$	$N_{\rm P}$	$\chi^2_{\rm DF}$	$N_{\rm P}$	$a_0^{I=0}$	$a_0^{I=2}$	$a_1^{I=1}$
	1.94	26	1.56	30	.04	-.151	-.016	1.58	31	1.46	32	.009	.15	-.040
	1.95	26	1.57	29	.03	-.155	-.011	1.58	32	1.46	32	.014	-.16	.020
								1.64	31	1.50	30	.136	-.12	.048
								1.66	31	1.51	33	.044	-.16	.048
										1.53	33	.045	-.20	.039
D	1.45	33	1.37	24	.16	-.084	.040	1.40	30	1.31	30	.14	-.14	.056
	1.45	25	1.40	30	.11	-.187	.064	1.42	38					
	1.45	27						1.42	36					
								1.44	31					
R	1.35	32	1.33	32	.11	-.004	-.026	1.25	37	1.22	36	.038	.015	.000
	1.36	31	1.33	33	.12	.002	-.025	1.38	37	1.35	39	.073	.0002	.008
			1.51	35	.18	-.138	-.012			1.40	34	.170	-.034	.028
N	1.42	23	1.39	27	.07	.004	-.014	1.36	33	1.32	30	.23	.052	.011
	1.42	22	1.39	28	.07	.004	-.014	1.37	27	1.32	30	.23	-.012	.018
			1.40	33	.16	.026	-.020	1.37	31	1.32	34	.14	-.012	.019
			1.41	28	.16	.023	-.020	1.37	28	1.33	29	.23	.029	.017
								1.37	27	1.33	26	.10	-.014	.015
D	1.25	34	1.25	30	.00	.000	.000	1.20	36	1.21	41	.13	-.026	.046
R	1.27	33	1.26	35	.19	-.058	.038	1.26	40	1.24	46	.12	-.105	.057
	1.29	35	1.26	35	.10	-.048	.033	1.26	39					
	1.33	38	1.31	43	.10	-.016	.026	1.28	38					
			2.01	40	.80	.21	.100							
D	1.31	31	1.29	32	.04	.025	.005	1.27	34	1.19	35	.11	.000	.045
N	1.31	32	1.30	32	.15	-.022	.023	1.29	34	1.24	31	.17	-.104	.048
	1.36	26						1.33	33					
R	1.24	29	1.23	36	.22	.037	-.035	1.19	35	1.15	43	.14	.042	-.008
N	1.34	39	1.31	36	.09	.009	-.015	1.32	45	1.29	40	.18	-.048	.005
	1.39	36	1.32	36	.20	-.047	.0002							
D	1.18	41	1.17	39	.05	-.027	.090	1.16	44	1.14	47	.15	.041	-.026
R	1.20	36	1.19	35	.02	.017	.005	1.18	41	1.15	46	.07	.025	.028
N	1.21	36	1.22	38	.27	.005	.028	1.19	40	1.16	42	.07	-.056	.045
	1.22	37	1.22	38	.05	-.029	.015	1.21	36	1.20	45	.07	-.076	.047
										1.20	41	.17	-.053	.054
										1.21	39	.19	-.059	.053

For illustrations we have chosen the solution from the "DRNbior" variant with $\chi^2_{\rm DF} = 1.16$ (see Table 5). The data on total cross sections and the theoretical curves in terms of the quasi–amplitude (15) are drawn in Fig. 2. The most intriguing feature of the discussed curves is expressed by the practical coincidence of the theoretical results for the $\{-\,0\,p\}$ and $\{+\,0\,p\}$ channels — this is clearly seen from the separate picture in Fig. 2 which we draw for the combined data. The picture makes it obvious that the discussed phenomenon is strongly implied by the experimental data. This means that the isotopic amplitude $\hat{D}$, being the only origin of the difference of the theoretical cross sections of these channels (see (9)), must vanish indeed.

At Figs. 3–8 one can find the theoretical curves of the same solution for the distribution data discussed in Sect. 3 in terms of the normalized quasi–amplitude (15). A part of the data did not enter the fittings — in such cases the curves actually represent our predictions — see Figs. 7, 8. The normalized quasi–amplitude measures the deviation from the empty–phase–space pattern. In its terms the behavior of the experimental data themselves appears to be quite different.

For example, almost all angular spectra of Figs. 5, 7 look flat. The explanation is simple: unlike the case of elastic reactions $2 \to 2$, the 1D distributions are given here by the remaining 3–dimensional phase space integrals of the $2 \to 3$ process. The averaging over polarizations together with this averaging over the reaction phase space make the angular dependence so weak. However, this can not be true for sections of the phase space and/or for higher dimensional distributions.

In contrast, the distributions in the invariant variables (7) are nontrivial — see Figs. 3, 4, 5, 6, 8; this proves the choice of variables of the paper [11] to be the characteristic one for the dynamics of the considered reaction.

The results of data analyses described in the current section make it possible to use the obtained amplitude

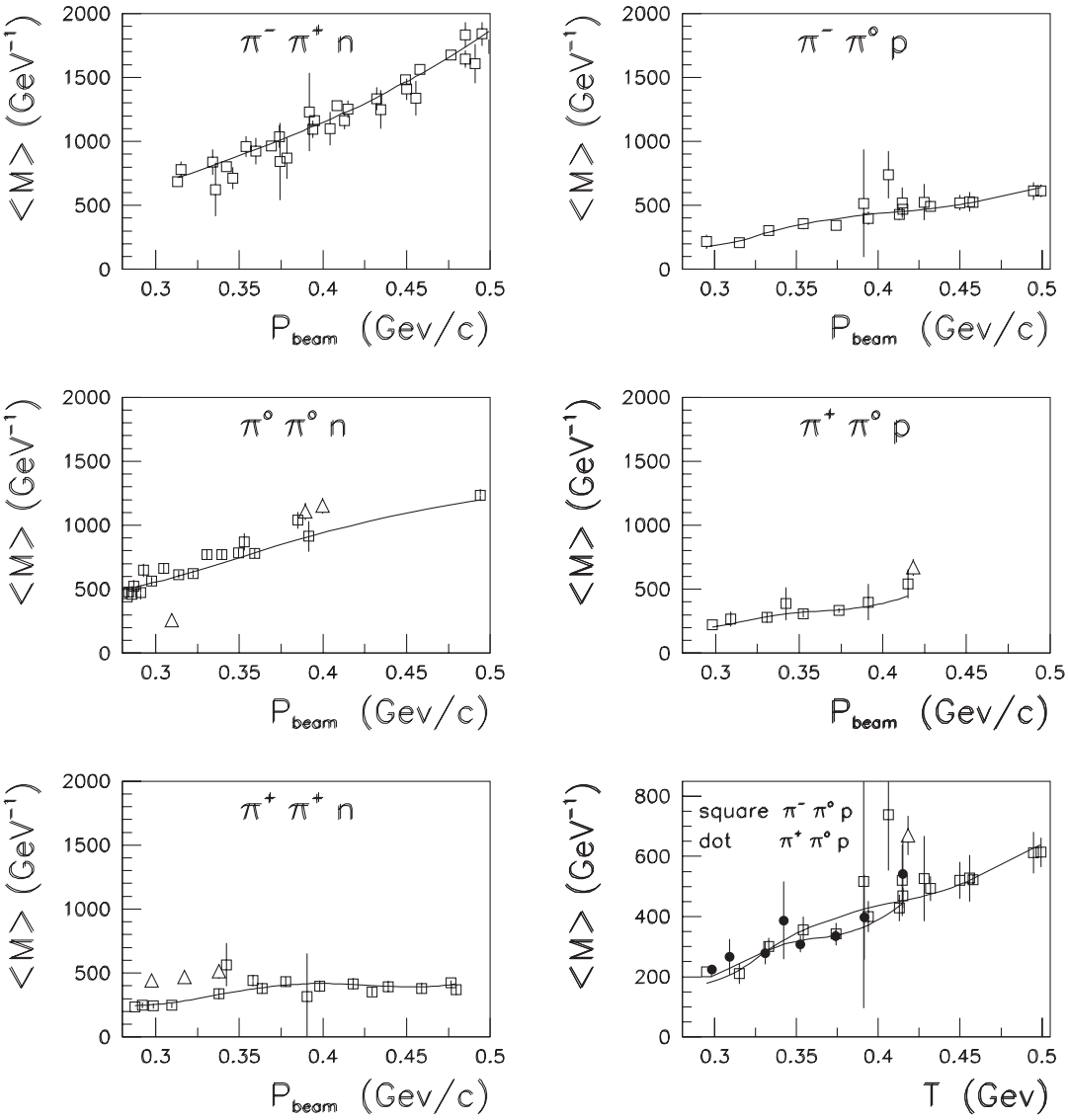

Fig. 2. Experimental points of total cross sections and the theoretical curve for the best physical solution (quasi–amplitude $\langle M \rangle$ in GeV^{-1}). *Triangle points* were excluded from fittings

for modeling two other approaches discussed in the Introduction, namely, the one by Olsson and Turner and the Chew–Low extrapolation. What we learn from these tests will be discussed in somewhere else.

5 Conclusions

Throughout the paper we were making the inferable statements along the discussions. Here, we remind the most important ones and develop the general conclusions.

5.1 Data

Our present work is devoted to the analysis of the near–threshold data on the $\pi 2\pi$ reaction. The data base described in Sect. 3. consists of the experimental total cross sections and 1–dimensional distributions. The full–kinematics data of the work [31] also had been presented in the same form. This needs some comments.

The available 1023 full–kinematics events of the quoted work constitute the solid ground for the total cross section; 10–14 bins of a 1–dimensional distribution have a good filling with the averaged number of 60–100 events per bin; the filling of 8×8 bins of a 2–dimensional distribution is satisfactory (15 events per bin in the average) while the filling of $6\times6\times6$ of the 3–dimensional ones and $4\times4\times4\times4$ of the 4–dimensional bins is poor. In this conditions of the difficult choice between the poor filling of bins and the loss of the kinematical information we formed multiple 1–dimensional projections for the data to bring to light the behavior in the crucial variables.

The use of the numerous lower dimensional distributions acts the part of a kind of the tomography method.

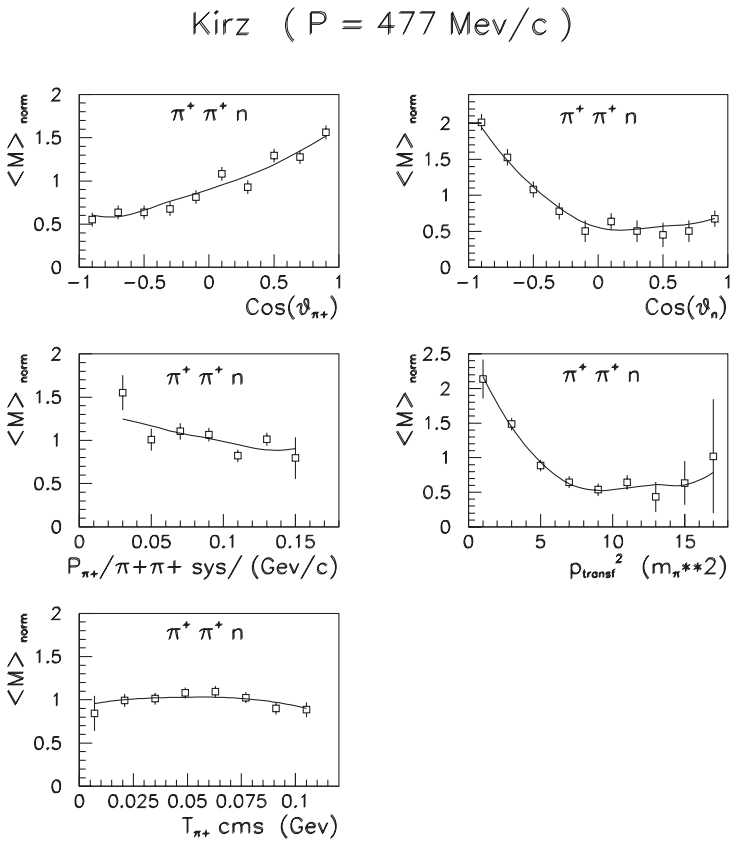

Fig. 3. Experimental distributions for the $\{++n\}$ channel from the paper [39] by Kirz and theoretical curves (normalized quasi–amplitude $\langle M\rangle_{\rm norm}$)

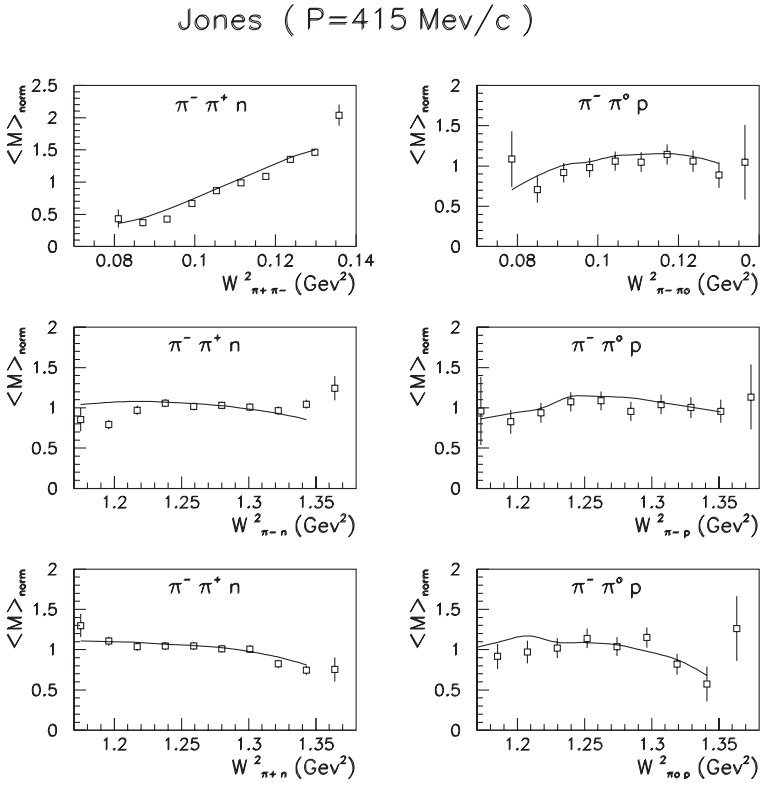

Fig. 4. Experimental distributions for the $\{-+n\}$ and $\{-0p\}$ channels from the paper [35] by Jones and theoretical curves (normalized quasi–amplitude $\langle M\rangle_{\rm norm}$)

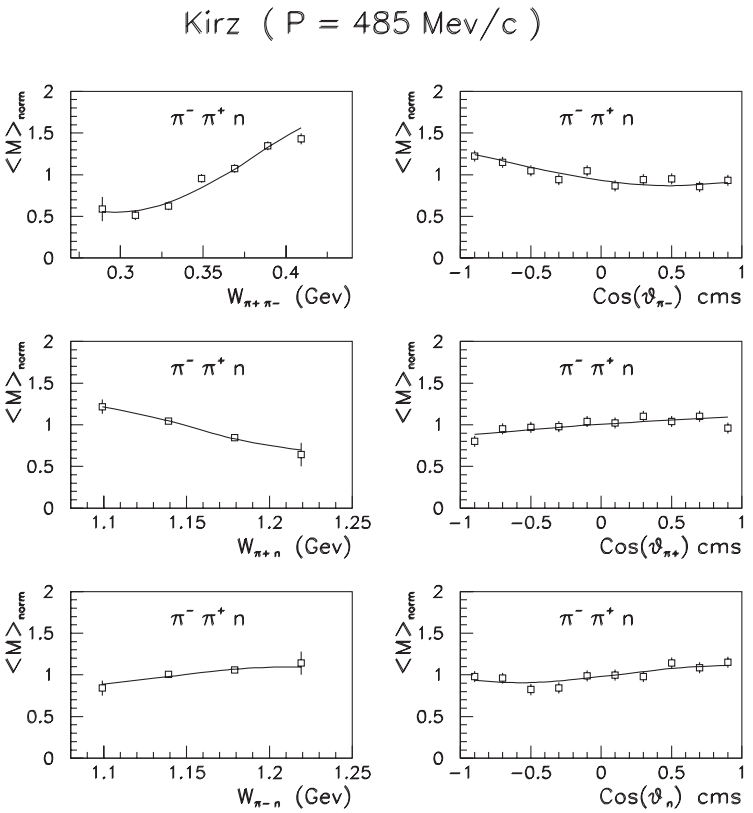

Fig. 5. Experimental distributions for the $\{-+n\}$ channel from the paper [40] by Kirz and theoretical curves (normalized quasi–amplitude $\langle M\rangle_{\rm norm}$)

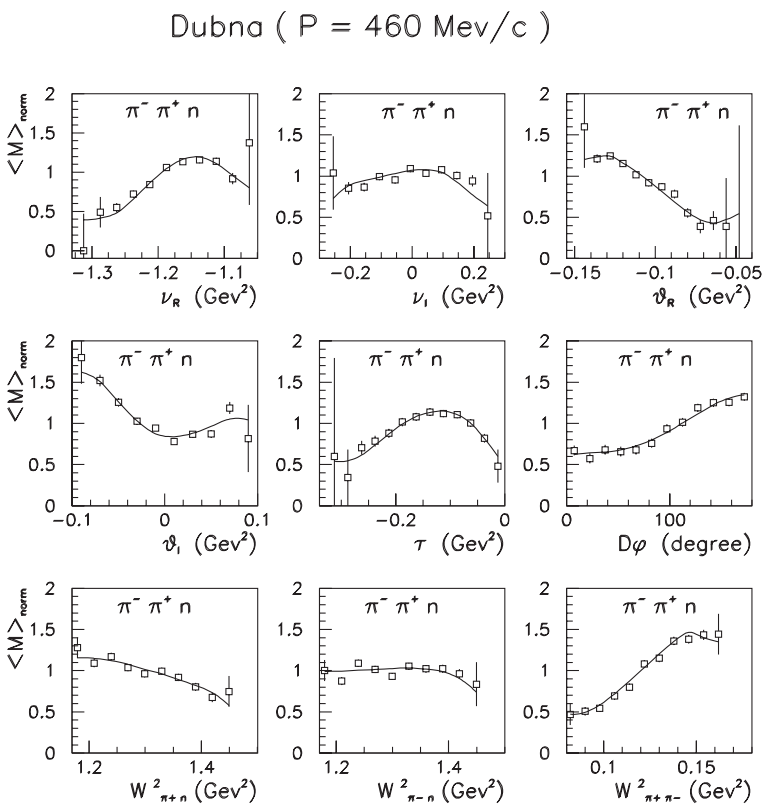

Fig. 6. Some of experimental distributions for the $\{-+n\}$ channel from the paper [31] by Blokhintseva and theoretical curves (normalized quasi–amplitude $\langle M\rangle_{\rm norm}$)

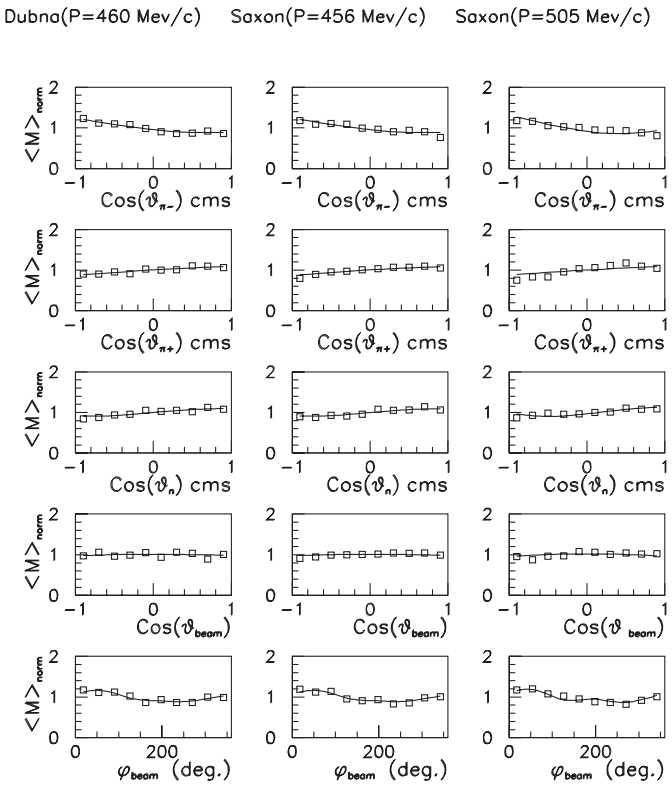

Fig. 7. Experimental distributions and theoretical curves for angular spectra of the $\{-+n\}$ channel from the Saxon's paper [46] and the same spectra build of the Blokhintseva data [31] (normalized quasi–amplitude $\langle M\rangle_{\rm norm}$). The Saxon data had not been used in fittings

The fittings showed that at a distance from resonance poles this works. We created some additional 1D projections of the data [31] and tested them with the obtained solutions — the description was found to be excellent. The improved statistics of the contemporary experiment [52, 9,53,54] definitely must make the direct use of the full–kinematics data more preferable.

The general properties of the treated data base are found to be:

1. The precision of data is insufficient to improve the accuracy of the determination of characteristics of the $\pi\pi$ scattering. However, this is the problem not only of the data.

2. The coverage of the behavior of the low energy amplitude is good; practically, there were no losses of convergence in the course of fittings. The existence of numerous solutions reflects the complexity of the reaction amplitude — the current experimental setup can not be charged for this; we shall continue this discussion below in the subsects. 5.2., 5.3.

3. The distribution data of the $\{++n\}$ channel are found to be extremely important for the resolution of parameter correlations. In the absence of these data the convergence of fittings becomes tremendously slow, the number of iterations being increased by several orders.

To resume we state that the considered data base is in principle sufficient for determination of the phenomenological near–threshold $\pi 2\pi$ amplitude. Certainly, the need in the better quality of data in respect to the precision of the obtained parameters and the multiplicity of solutions is obvious. First, the quality of the newest data will be much better and, second, it seems oversimplified to charge only the data with this problem. The more detailed discussion of its origin will be given in the next subsection.

5.2 Amplitude and major results

Our amplitude is built on the rather conservative basis. However, the orientation towards the modern ChPT approach in constructing the model might be lacking of an intrinsic tool for making the right explanation, if failed, whether an inconsistency of data or the neglect of higher order terms are responsible for the inappropriate fit. If successful, the approach provides the only conclusion that at the considered order ChPT is compatible with data — a substantial estimate of the systematic error of determination of the low energy constants is impossible.

The approach of HBChPT deserves the separate remark. Unlike the case of the πN–elastic scattering this approach is, probably, inapplicable to the case of the $\pi N \to \pi\pi N$ reaction considered here. One should remind the basic keystones of HBChPT: 1. Nonrelativistic limit; 2. Small–pion–momentum expansion; 3. Heavy baryon approximation. Then, let us consider the identity

$$\bar{u}(q)(\hat{k}_1 - \hat{k}_2 - \hat{k}_3)i\gamma_5 u(p) = -2m\,\bar{u}(q)i\gamma_5 u(p), \qquad (23)$$

which is specific to the relativistic form of the $\pi 2\pi$ amplitude. The identity can not support the above points 2., 3. simultaneously.

In the present paper we consider the amplitude of the $\pi 2\pi$ reaction built of numerous resonance contributions, including the separately treated OPE mechanism, and the smooth polynomial background (see Sect. 2.). Its complicated appearance reflects the influence of the, generally, off–shell processes like $\pi\pi \to \pi\pi$, $\pi N \to \pi N$, $\pi N \to \pi N^{(*)}$, $\pi N \to \pi\Delta$ on the near–threshold region of the discussed reaction.

The fittings strongly confirmed the importance of all quoted exchange mechanisms. This result can not be considered as the totally new one. For example, the importance of isobars already had been stressed in the paper [55] in terms of the sophisticated analysis of the amplitude form.

The near–threshold region $280 \le P_{\rm Lab} \le 500$ MeV/c can not be considered as the selfcontained one because of large Δ, $N^{(*)}$ widths. The isobars extend their strong influence up to the very $\pi 2\pi$ threshold. In the absence of isobar contributions the considerable improvement of the fit due to the imaginary background serves as an indirect evidence of the importance of the discussed isobar mechanisms (see Table 4). The interrelation of these mechanisms with the OPE one will be discussed below.

In view of the discussion of the role of background parameters (see Subsect. 2.4.) it is not so surprising that

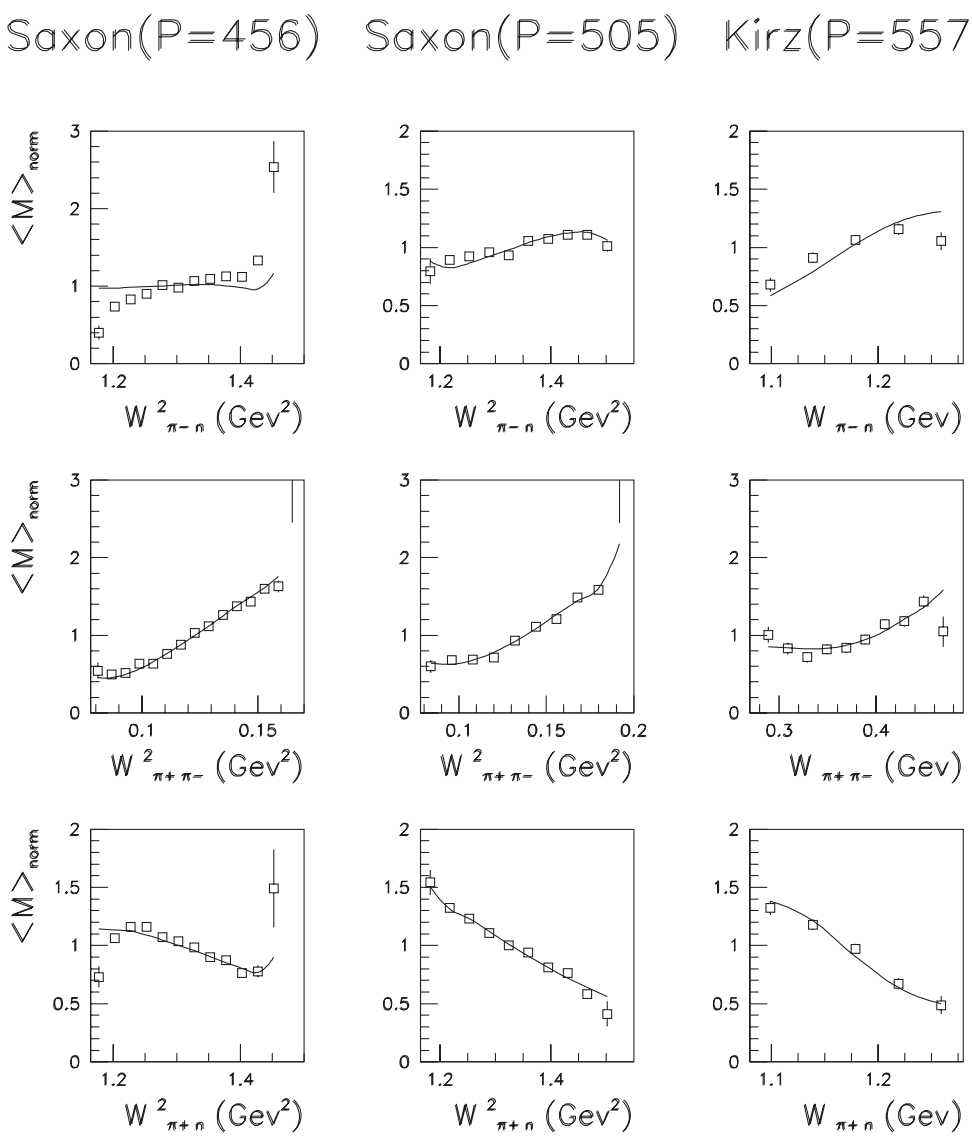

Fig. 8. Experimental distributions and theoretical predictions for spectra of the $\{- + n\}$ channel from the paper [46] by Saxon and from the paper [40] by Kirz (normalized quasi–amplitude $\langle M \rangle_{\rm norm}$)

only few of them are found important in fittings when all exchange mechanisms are being present. The fact that the parameters of the isospin amplitude D are found to be consistent with zero reflects the negligible influence of higher τ–resonances like $\mathrm{SE}_{NN}(\omega)$ on the amplitude in the considered energy region. Even the nonzero contributions to this isospin amplitude from isobar exchanges almost cancel each other — this might be derived from an approximate equality of the resulting theoretical cross sections of $\{-0p\}$ and $\{+0p\}$ channels.

The OPE contribution is in the center of our investigations. The improvement of $\chi^2_{\rm DF}$ with the inclusion of OPE is found to be statistically important in all variants (see Tables 4, 5). The 4π vertex of the OPE graph is taken in the direct amplitude form which contains 4 parameters g_0, g_1, g_2 and g_3 and respects the isospin, crossing and approximate–unitarity properties of the $\pi\pi$ amplitude off the mass shell. For values of these parameters in the best physical solutions in terms of the $\pi\pi$–scattering lengths see Table on the following page. Here, we list also the currently adopted experimental values of the compilation [50].

Generally, the solutions display that the precision of determination of the D–wave parameters g_2 and g_3 is not worse than that of g_0, g_1 parameters. This was attributed to the characteristic energy dependence of the isospin–zero S wave. The parameters of the latter via crossing and kinematics are related to D–wave scattering lengths — this is clearly demonstrated by the $a_2^{I=0}$ errors in the above list.

The poor precision of determination of the $\pi\pi$–interaction parameters has its origin in 3 principal reasons: 1) the data accuracy; 2) the competition of other mechanisms; 3) the incomplete nature of the current experimental setup.

The first point is evident — the data accuracy will be improved soon (look [4] for the survey of experiments).

The second one stems mainly from the isobar exchanges. This is clearly revealed by fittings: whenever an isobar mechanism is absent it is easy to find a solution with $a_0^{I=0}$ in the range 0.20 — 0.30; it drops to the 0.00 — 0.20 range

$\chi^2_{\rm DF}$	$a_0^{I=0}$	$a_0^{I=2}$	$a_1^{I=1}$	$a_2^{I=0}$	$a_2^{I=2}$
1.161	0.07±0.12	-0.056±0.036	0.045±0.017	0.0052±0.0031	-0. 0005±0.0014
1.203	0.07±0.11	-0.076±0.073	0.047±0.025	0.0023±0.0027	-0. 0013±0.0014
1.205	0.17±0.12	-0.053±0.039	0.054±0.022	0.0054±0.0025	-0. 0002±0.0012
1.212	0.19±0.11	-0.059±0.045	0.053±0.022	0.0062±0.0027	0. 0006±0.0015
[50]	0.26±0.05	-0.028±0.012	0.038±0.002	0.0017±0.0003	0.0001±0.0003

if all isobar mechanisms are involved. It is interesting that the effect of ρ exchanges is quite opposite. In other words, the larger values of $\pi\pi$–scattering lengths are gained when OPE is forced to stay for an essential but missed isobar contribution.

The important question is about the nature of parameters which correlations with the OPE set g_0, g_1, g_2, g_3 are so devastating. Unfortunately, these are not the parameters of the DE–type graphs which might be estimated from the decay characteristics or might be known, like the $g_{\pi NN}$ constant, from the low–energy πN phenomenology. Instead, the root correlations are due to parameters R_1–R_4 and D_1–D_4 of the $\mathrm{SE}_{\pi N}(N^{(*)})$, $\mathrm{SE}_{\pi N}(\Delta)$ graphs (see Tables 2, 3). The explanation is simple. Parameters of the graphs of the SE type play the same role in respect to the ones of the DE type as the background parameters A_1–A_{18} and their analogs i_{19}–i_{36} do in respect to all exchange parameters. Indeed, outside the resonance region the contraction of any pole in the DE graph leads to the single–pole contribution, i.e. to the one described by the SE graphs.

Here, one observes the interrelation of the point 2. with the first one since the data restricted to the region below resonances can not help much to fix up parameters of processes like $\pi N \to \pi N^{(*)}$, $N^{(*)} \to \pi\pi N$, $\pi N \to \pi\Delta$, etc.

We found the numerous set of solutions describing the data at the acceptable level of χ^2. The origin of this phenomenon must be explained in part by the importance of all 4 spin structures of the $\pi 2\pi$ amplitude (see (4), (10)). This is the reason number 3 for the poor accuracy of our final results.

Indeed, the unpolarized data measure only one combination of spin structures, namely, the combination given by the matrix element (14), leaving these structures almost free to stand one for another. Therefore, the absence of polarized measurements in the energy region $P_{\rm Lab} \approx$ 500 MeV/c and the abundance of mechanisms specific to the considered reaction is the reason of huge correlations of OPE parameters with the rest ones on the available data base.

Meanwhile, the extreme importance of the nucleon spin in the considered reaction at higher energies had been recently reported by Svec in the paper [56]. We see the clear signal of nontrivial spinor structures in the results of our analysis. This provides a motivation for the polarization measurements of $\pi N \to \pi\pi N$ reactions at the discussed energies. Up to now the known polarization measurements of the $\pi 2\pi$ reactions had been performed at considerably higher energies, for example, at 5.98 GeV/c and 11.85 GeV/c [57] and at 17.2 GeV/c [58]. Their analyses [59], [60] already proved such measurements to be detailed sources of information on the $\pi\pi$ interaction at high energies.

Certainly, the complete polarization experiment requires the analysis of the polarization of the final nucleon — in the near future this is hardly to be carried out for such rare processes as the considered one. Nevertheless, the examination of the spinor structure of the considered amplitude (4) displays that the almost exhaustive information might be obtained already from the experiment with the polarized target. Indeed, there are two independent asymetries

$$A_{\pm}(\mathbf{s}) = \frac{\sigma(\mathbf{s};\mathbf{k}_{\pm}^{\perp}) - \sigma(\mathbf{s};-\mathbf{k}_{\pm}^{\perp})}{\sigma(\mathbf{s};\mathbf{k}_{\pm}^{\perp}) + \sigma(\mathbf{s};-\mathbf{k}_{\pm}^{\perp})}, \qquad (24)$$

where $\mathbf{s}$ is the vector of the nucleon polarization and $\mathbf{k}_{\pm}^{\perp}$ are the projections of vectors $\mathbf{k}_{\pm} = \mathbf{k}_2 \pm \mathbf{k}_3$ to the plane which is orthogonal to $\mathbf{s}$. Their measurements must provide an information on two additional combinations of four spinor structures of the decomposition (4) which are independent from the combination of the matrix element (14).

5.3 General conclusion

We develop the phenomenological amplitude of the $\pi N \to \pi\pi N$ reaction taking into account the polynomial background derived with the account of isotopic, crossing, C, P and T symmetries of strong interactions, the exchanges of Δ and $N^{(*)}$ along with the OPE mechanism. The contribution of the latter contains 4 independent low energy parameters up to $O(k^4)$ order.

The data base consisting of total cross sections in the energy region $0.300 \le P_{\rm Lab} \le 500$ MeV/c and 1D distributions from the bubble–chamber experiments was used to determine free parameters of the amplitude. Practically all data points of the considered data base were found necessary for this.

For the first time there was found an amplitude equally well describing the broad variety of different data in all reaction channels. The best solutions are characterized by $\chi^2_{\rm DF} = 1.16$, $N = 411$. The isobar exchanges are found to be more important than OPE at the considered energies. Despite this the parameters of OPE are statistically significant; however, the $\pi\pi$–scattering lengths appear different in different solutions.

We find that the approach based on the extensive phenomenological model (*a la* Oset–Vicente–Vacas) requires to develop the common analyses of related processes like

$\pi N \to \pi N^{(*)}$, $\pi N \to \pi\Delta$ — i.e. the processes described by the Lagrangian terms listed in Tables 2, 3 — and, hence, to extend the energy region up to $P_{\rm Lab} \sim 1$ GeV/c. In other words, the problem of determination of the low–energy $\pi\pi$–scattering characteristics is a part of the more comprehensive problem of investigation of $\pi 2\pi$ dynamics at low and intermediate energies.

The results of contemporary experiments [53,54,52] must provide much more precise determination of $\pi\pi$ parameters since their correlations with the unknown parameters of isobar mechanisms originating from the discussed above spin structures will be resolved in part due to the improved data accuracy. However, it is difficult to over–estimate the role of the polarized data.

The amplitude which structure will be fixed by the analysis of statistically significant data, might gain the wide range of applications beyond the testing of ChPT predictions. For example, it might be used for the common analysis of $\pi N \to \pi\pi N$, $\gamma N \to \pi\pi N$ and πN–elastic data, for investigations of the η production in the process $\pi N \to \eta N$, for correcting experimental distributions obtained at devices with the restricted geometry and for other investigations at intermediate energies. This is ensured by the fundamental role of the $\pi N \to \pi\pi N$ reaction in nuclear and particle physics.

This research was supported in part by the RFBR grant N 95-02-05574a. We thank T.A. Bolokhov, P.A. Bolokhov, V.A. Guzey, A.N. Manashov, V.V. Vereshagin V.L. Yudichev, A.Yu. Zakharov for checking the formulae, testing the code and for other help at various stages of the project. We are grateful to P. Amaudruz, A. Bernstein, F. Bonutti, J. Brack, P. Camerini, G.A. Feofilov, E. Frlež, N. Grion, G. Hofman, R.R. Johnson, M. Kermani, M.G. Olsson, O.O. Patarakin, D. Počanić, R. Rui, M. Sevior, G.R. Smith for helpful discussions. We especially thank the CHAOS team for presenting computer powers of ALPHA stations at TRIUMF (Vancouver) and INFN (Trieste).

References

1. Knecht, M., Moussalam, B., Stern, J., and Fuchs, N.H., Nucl. Phys. B, **457** (1995) 513
2. Stern, J., Sazdjian, H., and Fuchs, N.H., Phys. Rev. D: Part. Fields, **47** (1993) 3814
3. Bijenes, J., Colangelo, G., Ecker, G., Gasser, J., and Sainio, M.A., Phys. Lett. B, **374** (1996) 210
4. Pocanic, D., Summary of π–π Scattering Experiments, in Bernstein, A.M., and Holstein, B.R., (eds.), Chiral Dynamics: Theory and Experiment, Proceedings of the Workshop held at MIT, Cambridge, MA, USA, 25–29 July (1994), Lecture Notes in Physics, LNP **452**, Springer–Verlag: Berlin and Heidelberg, (1995), 95
5. Lowe, J., Bassalleck, B., et al., Phys. Rev. C: Nucl. Phys., **44** (1991) 956
6. Počanić, D., Frlež, E., Assamagan, K.A., et al., Phys. Rev. Lett., **72** (1994) 1156
7. http://helena.phys.virginia.edu/˜pipin/E1179/E1179.html
8. http://helena.phys.virginia.edu/˜pipin/E857/E857.html
9. Smith, G.R., et al., Nucl. Instr. and Meth. A, **362** (1995) 349
10. Oset, E. and Vicente–Vacas, M.J., Nucl. Phys. A, **446** (1985) 584
11. Bolokhov, A.A., Vereshagin, V.V., and Sherman, S.G., Nucl. Phys. A, **530** (1991) 660
12. Bolokhov, A.A., Vereshchagin, V.V. and Sherman, S.G., Yad. Fiz., **45** (1987) 508; Sov. J. Nucl. Phys., **45** (1987) 319
13. Bolokhov, A.A., Sherman, S.G., and Vereshagin, V.V., Yad. Fiz., **46** (1987) 585
14. Rebbi, C., Ann. Phys. (NY), **49** (1968) 106
15. Manley, D.M., Phys. Rev. D: Part. Fields, **30** (1984) 536
16. Review of Particle Physics. Phys. Rev. D: Part. Fields, (1996), **54**, Number 1
17. Bolokhov, A.A., et al. Yad. Fiz., **60**N9 (1997) 1658–1668
18. Höhler, G., Pion–Nucleon Scattering, Landolt–Börnstein, New Series, ed. Schopper, Vol. I/9 b2 (Springer–Verlag, 1983)
19. Nath, L.M., Estemadi, B. and Kimel, J.D., Phys. Rev. D: Part. Fields, **3** (1970) 2153
20. Olsson, M.G. and Osypowski, E.T., Nucl. Phys. B, **101** (1975) 136
21. Donoghue, J.F., Golowich, E. and Holstein, B., Dynamics of the Standard Model, NY: Cambridge University Press, (1992)
22. Barish, B.C., Kurz, R.J., et al., Phys. Rev. B, **135B** (1964) 416
23. Batusov, Yu.A., Buniatov, C.A., et al., JETP, **40** (1961) 1528
24. Batusov, Yu.A., Buniatov, C.A., et al., Yad. Fiz., **1** (1965) 562, 687
25. Batusov, Yu.A., Buniatov, C.A., et al., Yad. Fiz., **18** (1973) 86
26. Batusov, Yu.A., Buniatov, C.A., et al., Yad. Fiz., **21** (1975) 308
27. Belkov, A.A., Buniatov, C.A., et al., Yad. Fiz., **31** (1980) 181
28. Bjork, S.W., Jones, S.E., et al., Phys. Rev. Lett., **44** (1980) 62
29. Blair, I.M., Muller, H., Torelli, G., Zavattini, E., Physics Lett. B, **32** (1970) 528
30. Blokhintseva, T.D., Grebinnik, V.G., et al., JETP, **44** (1963) 498
31. Blokhintseva, T.D., Kravtsov, A.V., et al., Yad. Fiz., **12** (1970) 101-108; Sov. Journ. Nucl. Phys, **12** (1971) 55
32. Buniatov, C.A., Kurbatov, V., et al., Nucl. Phys. B, **42** (1972) 77
33. Buniatov, C.A., Jolobov, G.V., et al., Yad. Fiz., **25** (1977) 325
34. Deahl, J., Derrick, M., et al., Phys. Rev., 1961, **124**, (1987)
35. Jones, J.A., Allison, W.W.M., Saxon, D.H., Nucl. Phys. B, **83** (1974) 93
36. Kernel, G., Korbar, D., et al., Phys. Lett B, **216** (1989) 244
37. Kernel, G., Korbar, D., et al., Phys. Lett B, **225** (1989) 198
38. Kernel, G., Korbar, D., et al., Z. Phys. C, **48** (1990) 201
39. Kirz, J., Schwartz, J., Tripp, R.D., Phys. Rev., **126** (1962) 763
40. Kirz, J., Schwartz, J., Tripp, R.D., Phys. Rev., **130** (1963) 2481
41. Kravtsov, A.V., Nemenov, L.L., et al., Yad. Fiz., **20** (1974) 942

42. Kravtsov, A.V., Lobachov, E.A., et al., Nucl. Phys. B, **134** (1978) 413
43. Perkins, W.A., Caris, J.C., Kenney, R.W., Perez-Mendez, V., Phys. Rev., **118** (1960) 1364
44. Sevior, M.E., Ambardar, , et al., Phys. Rev. Lett., **66** (1991) 2569
45. Sober, D.I., Arman, M., et al., Phys. Rev. D: Part. Fields, **11** (1975) 1017
46. Saxon, D.H., Mulvey, J.H., Chinowsky, W., Phys. Rev. D: Part. Fields, **2** (1970) 1790
47. Vereshagin, V.V., Sherman, S.G., et al., Nucl. Phys. A, **592** (1995) 413
48. Hern, A.C., *REDUCE User's Manual*, Santa Monica: Rand Corp., (1985)
49. Bolokhov, A.A., Bolokhov, P.A., Bolokhov, T.A. and Sherman, S.G., *Gauss Integration over Relativistic 3–Body Phase Space for 1–Dimensional Distributions of* $2 \to 3$ *Reaction*, preprint hep-ph/9601264; *SPbU-IP-96-1*, Sankt-Petersburg, (1996), 32p
50. Dumbrais, O., et al., Nucl. Phys. B, **216** (1983) 277
51. Gasser, J. and Leutwyler, H., Phys. Lett B, **125** (1982) 312; Phys. Lett B, **125** (1982) 325
52. Smith, G.R. and Kermani, M., Experiment 624: The $(\pi, 2\pi)$ reaction, a tool to determine scattering lengths and coupling constants, TRIUMF Annual Report Scientific Activities (1994), Vancouver: TRIUMF, (1994), 23
53. Kermani M.A., First results of exclusive measurements of $\pi N \to \pi\pi N$ with CHAOS detector, in Bernstein, A.M., and Holstein, B.R., (eds.), Chiral Dynamics: Theory and Experiment, Proceedings of the Workshop held at MIT, Cambridge, MA, USA, 25–29 July (1994), Lecture Notes in Physics, LNP vol. 452, Springer–Verlag: Berlin and Heidelberg, (1995), 115
54. Sevior, M.E., Preliminary results of a new measurement of the reaction $\pi^+ p \to \pi^+\pi^+ n$ near threshold, in Bernstein, A.M., and Holstein, B.R., (eds.), Chiral Dynamics: Theory and Experiment, Proceedings of the Workshop held at MIT, Cambridge, MA, USA, 25–29 July (1994), Lecture Notes in Physics, LNP vol. 452, Springer–Verlag: Berlin and Heidelberg, (1995), 114
55. Johnson, R.R., Fasel, N. and Suen, N., πN–Newsletter, **8** (1993) 121
56. Svec, M., Phys. Rev. D: Part. Fields, **55** (1997) 4355
57. A.de, Lesquen, et al., Phys. Rev. D: Part. Fields, **32** (1985) 21
58. Grayer, G., et al., Nucl. Phys. B, **75** (1974) 189
59. Svec, M., Phys. Rev. D: Part. Fields, **46** (1992) 949
60. Becker, H., et al., Nucl. Phys. B, **151** (1979) 46